arXiv:1610.08901v1 [cond-mat.mes-hall] 27 Oct 2016

Spin Currents and Magnon Dynamics in Insulating Magnets

Kouki Nakata,[1] Pascal Simon,[2] and Daniel Loss[1]
[1] *Department of Physics, University of Basel, Klingelbergstrasse 82, CH-4056 Basel, Switzerland*
[2] *Laboratoire de Physique des Solides, CNRS UMR-8502, Université Paris Sud, 91405 Orsay Cedex, France*

(Dated: October 28, 2016)

Nambu-Goldstone theorem provides gapless modes to both relativistic and nonrelativistic systems. The Nambu-Goldstone bosons in insulating magnets are called magnons or spin-waves and play a key role in magnetization transport. We review here our past works on magnetization transport in insulating magnets and also add new insights, with a particular focus on magnon transport. We summarize in detail the magnon counterparts of electron transport, such as the Wiedemann-Franz law, the Onsager reciprocal relation between the Seebeck and Peltier coefficients, the Hall effects, the superconducting state, the Josephson effects, and the persistent quantized current in a ring to list a few. Focusing on the electromagnetism of moving magnons, i.e., magnetic dipoles, we theoretically propose a way to directly measure magnon currents. As a consequence of the Mermin-Wagner-Hohenberg theorem, spin transport is drastically altered in one-dimensional antiferromagnetic (AF) spin-1/2 chains; where the Néel order is destroyed by quantum fluctuations and a quasiparticle magnon-like picture breaks down. Instead, the the low-energy collective excitations of the AF spin chain are described by a Tomonaga-Luttinger liquid (TLL) which provides to the spin transport properties in such antiferromagnets some universal features at low enough temperature. Finally, we enumerate open issues and provide a platform to discuss the future directions of magnonics.

PACS numbers: Review article for special issue on magnonics from J. Phys. D.

I. INTRODUCTION

Symmetry and its spontaneous breaking are fundamental concepts to understand and classify the low-energy physics of many systems. The Nambu-Goldstone theorem[1–3] ensures that when a continuous symmetry is spontaneously broken, gapless modes appear. The massless[4–8] modes are called Nambu-Goldstone bosons and their energy vanish in the long wavelength limit $k \to 0$. The dispersion becomes linear in Lorentz-invariant (i.e., relativistic) systems, while it may be nonlinear in nonrelativistic systems and varies from one system to another (see Refs. [9,10]). Well-known examples in solids are the so-called magnons[11,12] or spin-waves (Fig. 1). On cubic lattices, the low-energy physics is characterized by nonrelativistic-like magnons with a quadratic dispersion in ferromagnets (FMs), while relativistic-like magnons emerge in antiferromagnets (AFs) where the Néel order is developed.

The situation changes in lower dimensions $\mathcal{D} \leq 2$. The Mermin-Wagner-Hohenberg theorem[13,14] prohibits the spontaneous breaking of continuous symmetries at finite temperature in the thermodynamics limit (see Ref. [15] for an extension). Therefore, spontaneous magnetic orders in $\mathcal{D} \leq 2$ spin systems are generally not possible at any finite temperature. Indeed, the Néel order is destroyed by quantum fluctuations (i.e. strong quantum effects) in one-dimensional antiferromagnetic spin-1/2 chains and the quasiparticle picture (*e.g.*, magnon) breaks down; instead the low-energy physics is described by the Tomonaga-Luttinger liquid[16,17] (TLL).

The dimensionality thus plays a crucial role on magnetism. We summarize here spin transport properties in $\mathcal{D}$ dimensions, with a particular focus on magnons transport in insulating bulk magnets. Quantum-statistical mechanics provides two kinds of particles; bosons and fermions. Electrons are fermions bounded by the Pauli exclusion principle, while magnons are bosons free from it. One may think at first sight that this drastic difference in statical properties of these excitations will lead to strong differences between magnon and electron transport. In this paper, we instead describe many magnon counterparts of electron transport (see Table I for a comparison). We review our past works on spin transport in insulating magnets and also add new insights to it[18–31].

The bosonic nature of magnons enables, however, excited magnons to dynamically condensate[32]. We then reveal the resulting transport properties[28,29] analogous to supercurrents of superconductors and summarize our recent results on universal thermomagnetic relations[30] in insulating magnets. We also provide a platform to discuss the next direction of magnon spintronics, dubbed magnonics[33–38], based on fundamental physics (see Refs. [33,34] for some applications).

The paper is organized as follows. In Sec. II, considering quasi-one-dimensional spin chains of finite size, we describe the spin transport carried by magnons in FMs and the one by TLL in AFs, and reveal the intrinsic properties to one-dimensional AFs. In Sec. III, introducing a Berry phase particular to magnetic dipoles, we demonstrate that it generates phenomena analogous to Hall effects in two-dimensional magnets [*e.g.*, ferromagnetic insulators (FIs)]. In Sec. IV, focusing on a three-dimensional ferromagnetic insulating junction, we discuss the transport properties of both non-condensed and condensed magnons, and clarify the differences; after reviewing fundamentals of magnons in Sec. IV A, we consider the magnon and heat transport, and find

TABLE I: Magnon analogues of electron transport. Spin Seebeck[39–41] and Peltier[42] effects in a metal/FI junction were observed by the inverse spin Hall effect[43], and the Onsager relation between them and the deviation were observed in Ref. [44]. Ref. [45] reported the observation of magnonic thermal Hall effect[46] and magnonic Snell's law has been experimentally established in Ref. [47]. See Ref. [48] for a WF law of spin transport in one-dimensional integrable spin-1/2 XXZ chain[49] and Refs. [50–54] for the progress[55] on the WF laws of non-Fermi liquids. A spinon spin current in one-dimensional spin-1/2 chain has been observed in Ref. [56]. Refs. [57,58] have theoretically proposed magnon spin Nernst effects in antiferromagnets[59–61].

Electron transport[62] e	Magnon transport $\mu_{\rm m}$
Electric current	Spin-wave spin current[63]
Seebeck effect	Spin Seebeck effect[39–41,64–69]
Peltier effect	Spin Peltier effect[42,70]
Wiedemann-Franz law[71]	Magnonic Wiedemann-Franz law[30]
Superconductive state	Quasiequilibrium magnon condensate[32,72]
Josephson effect[73]	Magnon Josephson effect[28]
Persistent current:	'Persistent' current[28] of quasiequilibrium condensates:
Quantization in superconducting ring (i.e., fluxoid)	Quantization in magnon condensate ring[28]
Electronic quantum RC circuit[74–78]	Magnetic quantum RC circuit[23]
Electronic transistor	Magnon transistor[24,79]

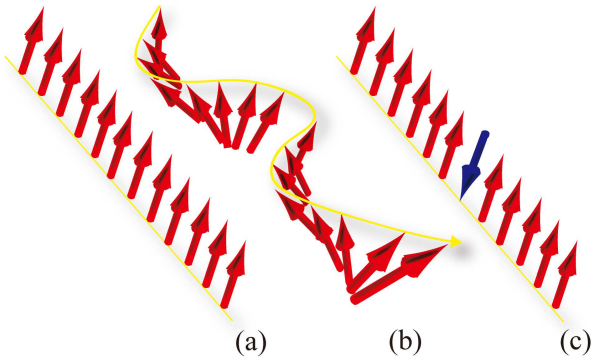

FIG. 1: (Color online) Schematic representation of a spin-wave, which characterizes a low-energy excitation in magnets. Its quantum counter part corresponds to a magnon excitation. Such a Nambu-Goldstone boson appears by the spontaneous symmetry breaking [*e.g.*, $SO(3) \mapsto SO(2)$ in (a)] and its dispersion vanishes in the long wavelength limit $k \to 0$ (i.e., a gapless collective mode). Assuming the exchange interaction $J > 0$ between the nearest neighboring spins of a ferromagnet with lattice constant a, we denote by $E_{\rm a,b,c)}$, the energy of (a) the spin polarized state, (b) the spin-wave state, and (c) the spin-flip state, respectively. These energies can be estimated as follows; $\delta E_{\rm ba} \equiv E_{\rm b} - E_{\rm a} = \mathcal{O}(Ja^2k^2) \to 0$ when $k \to 0$, $\delta E_{\rm ca} \equiv E_{\rm c} - E_{\rm a} = \mathcal{O}(J)$, and $\delta E_{\rm ba}/\delta E_{\rm ca} = \mathcal{O}(a^2k^2) \ll 1$ in the long wavelength limit.

the universal thermomagnetic relation in Sec. IV B. The magnon states are classified in detail and the resulting transport properties, represented by Josephson effects *etc.*, are summarized in Sec. IV C. The persistent current and the quantization are discussed in Sec. IV D, and we theoretically propose how to directly measure it in Sec. IV E based on the electromagnetism of magnetic dipoles. Finally, we summarize in Sec. V and enumerate open issues in Sec. VI.

II. SPIN TRANSPORT IN SPIN CHAINS

The Mermin-Wagner theorem[13–15] prohibits the spontaneous magnetic order in $\mathcal{D} \leq 2$ isotropic spin systems at finite temperature (with sufficiently short-ranged exchange coupling), but only in the thermodynamic limit; effective ordering in nanostructures of a finite size at sufficiently low temperatures is possible. We then consider a quasi-one-dimensional spin chain of a finite length and investigate the magnetization transport both in FMs and AFs.

A. Spin Conductances

We consider[21] a quasi-one-dimensional spin system illustrated in Fig. 2. The spin chain of finite length L is sandwiched between two bulk (i.e., large three-dimensional) magnets which work as reservoirs for magnetization. The reservoirs narrow adiabatically around the transition regions $\mid x \mid \approx L/2$ and are connected to the chain. A small spatially varying magnetic field $\delta B(x)\mathbf{e}_z$ is superimposed on the offset field $B\mathbf{e}_z$ with (Fig. 2)

$$\delta B(x) = \begin{cases} -\Delta B/2 & \text{for } \ x < -L/2, \\ \Delta B/2 & \text{for } \ x > L/2, \end{cases} \tag{1}$$

which interpolates smoothly through the region $\mid x \mid < L/2$ between the values $\pm\Delta B/2$ in the reservoirs (see Ref. [21] for details). These extra-fields $\pm\Delta B/2$ act like chemical potentials and need to be kept constant by a spin battery and/or by spin-lattice relaxation processes which keep the magnon occupation number at a constant value corresponding to the lattice temperature and Zeeman energy in each reservoir. Thus, a chemical potential difference acts then like a force on the magnons and drives a current of magnons. The flow of magnons from one reservoir to the other should be slow compared to

the time it takes to refill the leaving/arriving magnons in each reservoir. The field gradient (acting like a chemical potential gradient) produces a magnetization current $I_{\rm m}$ from the left to the right reservoir

$$I_{\rm m} = G_S \Delta B, \tag{2}$$

where G_S is the spin conductance; like for electrons[80], it remains finite in the ballistic limit due to the contact resistance between the reservoirs and the chain[21].

The spin chain extends from $x = -L/2$ to $L/2$ and it is described by

$$H_{\rm chain} = J \sum_{\langle ij \rangle} \mathbf{S}_i \cdot \mathbf{S}_j + g\mu_{\rm B} \sum_i B_i S_i^z, \tag{3}$$

where $J < 0$ is the exchange interaction between the nearest neighbor spins $\mathbf{S}_i$ and $\mathbf{S}_j$ on sites i, j for FMs and $J > 0$ for AFs. The magnetization is characterized by[12,81] magnons in a FM, while for spin-1/2 AF chain it can be mapped to spinless fermions via Jordan-Wigner transformation which can then be bosonized to give rise Tomonaga Luttinger Liquids (TLLs)[82–85].

We arrange the spin chains in parallel. Assuming a weak intermediate exchange interaction $J_{\rm inter}$ between the spin chains $|J_{\rm inter}| \ll |J|$, they can be regarded as being uncoupled with each other at temperatures $|J_{\rm inter}| \ll k_{\rm B}T \ll |J|$. Linear response theory provides the spin conductances (see Ref. [21] for details)

$$G_S = N_{\rm chain} \frac{(g\mu_{\rm B})^2}{h} \begin{cases} n_{\rm B}(g\mu_{\rm B}B) & \text{for FM,} \\ 1/K_b & \text{for AF,} \end{cases} \tag{4}$$

where $N_{\rm chain}$ is the number of spin chains, the Bose distribution function $n_{\rm B}(\epsilon) = 1/[\exp(\epsilon/k_{\rm B}T) - 1]$, and the interaction parameter K_b in the reservoirs; it becomes $K_b \approx 1$ for isotropic antiferromagnetic bulk reservoirs (and $K_b = 1$ for an XY AF).

B. Power Dissipation

Assuming that the spin chain $H_{\rm chain}$ [Eq. (3)] and the magnetic reservoirs in Fig. 2 consist of AFs ($J > 0$), we[22] generalized the above theory to the response to an ac magnetization source where the magnetic field bias ΔB (Fig. 2) changes periodically in time at a given driving frequency ω: Eq. (1) is replaced by

$$\delta B(x) = \begin{cases} -(\Delta B/2)\cos(\omega t) & \text{for } x < -L/2, \\ (\Delta B/2)\cos(\omega t) & \text{for } x > L/2, \end{cases} \tag{5}$$

and the oscillating magnetic field produces the magnetization current $I_{\rm m}$ in a XXZ spin chain described by

$$H_{XXZ} = J \sum_{\langle i,j \rangle} (S_i^x S_j^x + S_i^y S_j^y + \Delta S_i^z S_j^z), \tag{6}$$

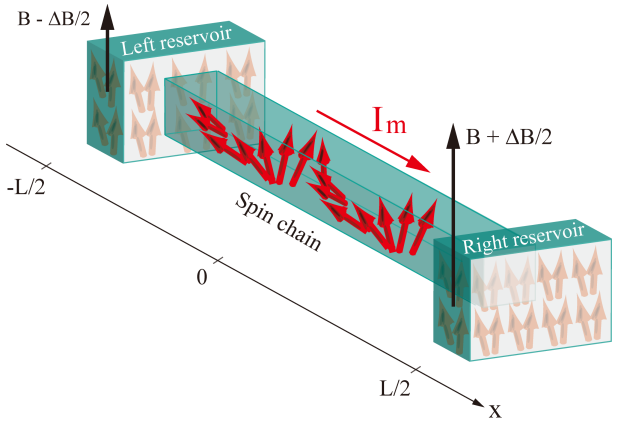

FIG. 2: (Color online) Schematic representation of a spin chain with a finite length L sandwiched between two large three-dimensional magnetic reservoirs. A small spatially varying magnetic field [Eq. (1)] is superimposed on the offset field $B\mathbf{e}_z$, which interpolates smoothly between the values $\pm\Delta B/2$ in the reservoirs. The field gradient produces a magnetization current $I_{\rm m} = G_S \Delta B$. The setup was proposed in Ref. [21].

where we assume $J, \Delta > 0$ namely antiferromagnetic interactions. Again, the low-energy effective theory of the spin Hamiltonian H_{XXZ} is given by a TLL,

$$H_{\rm TLL} = \frac{\hbar v}{2} \int dx \Big[g_{\rm TLL} [\Pi(x)]^2 + [\partial_x \varphi(x)]^2 / g_{\rm TLL} \Big], \tag{7}$$

where $g_{\rm TLL} \equiv (1 + 4\Delta/\pi)^{-1/2}$ denotes the Luttinger interaction parameter and v the velocity of the spinon excitation. We also introduced the Bose field operator $\varphi(x)$ in the bosonization language associated with spinon excitations and its conjugate momentum density $\Pi(x)$. Note that we have ignored Umklapp scattering in Eq. (7). A non-interacting system corresponds to $g_{\rm TLL} = 1$ (i.e. $\Delta = 0$). The reservoirs can also be described within this formalism by introducing an inhomogeneous TLL. This amounts to assign a spatial dependence to v and $g_{\rm TLL}$ such that $v(x) = v_r$ and $g_{\rm TLL}(x) = g_r$ in the reservoirs (for $|x| > L/2$) and $v(x) = v_c$, $g_{\rm TLL}(x) = g_c$ in the spin chain region (for $|x| < L/2$). We typically expect $g_r \approx 1$. Within this formalism, the magnetization current $I_{\rm m}(\omega)$ and the spin conductance G_S [Eq. (2)] can be evaluated using linear response theory (see Refs. [21,22] for details).

Then the magnetic power $W_{\rm m}(\omega)$ is defined by $W_{\rm m}(\omega) \equiv I_{\rm m}^2(\omega)/(2G_S)$ in analogy to the electric power (i.e., Joule heating) $W_{\rm e} \equiv I_{\rm e}^2/(2G_{\rm e})$, where $I_{\rm e}$ is an electric current, $G_{\rm e}$ the conductance , and ΔV an external voltage difference. The finite frequency absorption power can be expressed as[22]

$$W_{\rm m}(\omega) = g_c \frac{(g\mu_B \Delta B)^2}{2h} \left(\frac{\sin(\tilde{\omega}/2)}{\tilde{\omega}/2} \right)^2 \times \frac{1 - \gamma^4 + 2\gamma(1-\gamma^2)\cos(\tilde{\omega})}{1 + \gamma^4 - 2\gamma^2 \cos(2\tilde{\omega})}, \tag{8}$$

TABLE II: Geometric phases for electrons of charge e and magnons of magnetic moment $\mu_{\rm m}$ moving along a path γ for the geometry under consideration. Both are special cases of the Berry phase[86,87]. Moving magnons in electric fields $\mathbf{E}$ acquire the A-C phase $\theta_{\text{A-C}}$, which is analogous to the A-B phase[61,88] $\theta_{\text{A-B}}$ for electrons. The Dzyaloshinskii-Moriya (DM) interaction[45,89–92] acts as an electric vector potential and can be identified[93–95] with the A-C effect.

Aharonov-Bohm (A-B) phase[96]	Aharonov-Casher (A-C) phase[97]
Particle with electric charge e	Magnon with magnetic dipole moment $\mu_{\rm m} = -g\mu_{\rm B}\mathbf{e}_z$
Magnetic vector potential $\mathbf{A}$	Electric 'vector potential' $\mathbf{A}_{\rm m} \equiv \mathbf{E} \times \mu_{\rm m}$
$\theta_{\text{A-B}} = [e/(\hbar c)] \int_\gamma \mathrm{d}\mathbf{l} \cdot \mathbf{A}$	$\theta_{\text{A-C}} = [g\mu_{\rm B}/(\hbar c^2)] \int_\gamma \mathrm{d}\mathbf{l} \cdot (\mathbf{E} \times \mathbf{e}_z)$

where $\gamma = (g_r - g_c)/(g_r + g_c)$ is the reflection coefficient of spinon excitations at the sharp boundary between the chain and its reservoirs and $\tilde{\omega} = \omega L/v_c$ the ratio between the frequency and level spacing in the finite size chain. Note in passing that a measurement of the absorbed power due to ac excitation of the quantum spin chain provides a way to measure interaction dependent coefficients such as g_c. Another conclusion can be drawn from Eq. (9): we notice that $W_{\rm m}(\omega)$ vanishes as $(\sin(\tilde{\omega}/2))^2$ close to $\omega \approx 2\pi nL/v_c$ with n integer. One can show instead that the spin current resulting from a continuous wave radiation vanishes only as $\sin(\tilde{\omega}/2)$ close to that driving frequency. This implies that the magnetic power absorption is more strongly suppressed than the magnetization current at frequencies close to $2\pi nL/v_c$. This feature could be used to transfer a spin current (thus data) at special frequencies with low power dissipation.

In the limit $\omega \to 0$, Eq. (9) reads

$$W_{\rm m} = g_r(g\mu_{\rm B}\Delta B)^2/(2h), \tag{9}$$

to be compared with the typical electric power $W_{\rm e} = (e\Delta V)^2/h$. Let us now give estimate of these two powers consumptions. For typical values $\Delta V = 1$mV and $\Delta B = 0.1$T, we find

$$W_{\rm m} = \mathcal{O}(10^{-15})\text{J}/s \approx 10^{-4}W_{\rm e}, \tag{10}$$

where $g_r = 1$ was assumed. We can thus conclude that substantial advantages with respect to power consumption can be found using spin magnetization currents in insulators instead of electric currents.

C. Quantum Magnetic RC Circuit

By analogy with quantum optics where the single-photon source is a major element to encode or manipulate a quantum state[98], or with quantum electronics where an on-demand electron source has been recently realized[99–101], we have recently proposed how to realize some on-demand single magnon or spinon excitations using magnetic insulators.[23]

In analogy to the charged-based quantum RC circuit[74–78] (Table I), we proposed a quantum magnetic RC circuit as depicted in Fig. 3 that could potentially act as an on-demand coherent source of magnons or spinons.[23] In Fig. 3 the magnetic dot is weakly exchange coupled to a large magnetic reservoir and both of them are assumed to be nonitinerant magnets. We describe these insulating magnets by a Heisenberg Hamiltonian for one-dimensional spin chains (see Ref. [23] for details). A static-and time-dependent component of magnetic field $B_D(\omega)$ is applied to the dot and the excess magnetization of the magnetic dot $M_D(\omega)$ is characterized by

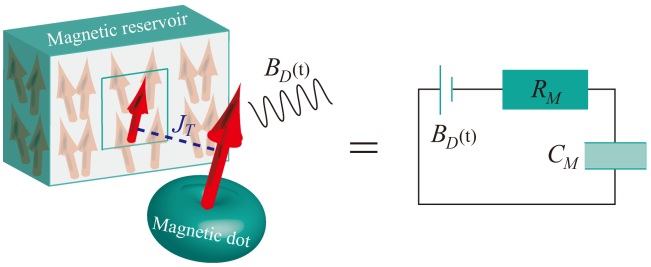

FIG. 3: (Color online) Schematic representation of a quantum magnetic RC circuit proposed in Ref. [23], which consists of the magnetic resistance R_M, the capacitance C_M, and the applied magnetic field B_D. The magnetic dot and the reservoir are weakly coupled by the exchange interaction J_T and both of them are modeled as one-dimensional chains.

$$\frac{M_D(\omega)}{B_D(\omega)} = C_M(1 + i\omega C_M R_M), \tag{11}$$

where R_M and C_M are the magnetic resistance and the capacitance respectively of the equivalent RC circuit (see Fig. 3). The excess magnetization is defined as $M_D(\omega) = g\mu_B N_D(\omega)$, where $N_D(\omega)$ is the Fourier transform of the time-dependent excess number of magnetic quantum excitations (magnons or spinons) in the dot magnetic insulator. We describe both the magnetic dot and the reservoir by spin chains. They can be both modeled by the spin anisotropic Heisenberg Hamiltonian. The magnetic dot Heisenberg Hamiltonian reads

$$H_D = \sum_{\langle ij \rangle} \mathbf{S}_i \cdot \mathbf{J}_D \cdot \mathbf{S}_j + g\mu_B \sum_i \mathbf{B}_D(t) \cdot \mathbf{S}_i. \tag{12}$$

$\mathbf{J}_D$ denotes a diagonal 3×3-matrix with $\text{diag}(\mathbf{J}_D) = J_D\{1, 1, \Delta_D\}$. J_D is the magnitude of the exchange interaction and Δ_D the anisotropy in our model. $J_D \lessgtr 0$ corresponds respectively to the FM and the AF ground

state. The field $\mathbf{B}_D(t) = B_D(t)\mathbf{e}_z$ denotes the time-dependent magnetic field applied to the dot. A similar Hamiltonian can be used to describe the reservoir (introducing different coupling constants) with only a constant magnetic field.

We couple these two systems, the magnetic dot and the reservoir, via some exchange interaction of the form $J_T\mathbf{S}_R \cdot \mathbf{S}_D$, where $\mathbf{S}_R$ is the last spin in the reservoir and $\mathbf{S}_D$ the first spin in the dot.

Using the linear response theory, we can express the change in magnetization $M_D(\omega)$ due to a small time-dependent change in $B_D(\omega)$ in terms of the density retarded Green function, $M_D(\omega) = (g\mu_B)^2 G_{\rm ret}(\omega)B_D(\omega)$ where $G(\omega) = i\int_0^\infty dt e^{i\omega t}\langle \hat{N}_D(t)\hat{N}_D(0)\rangle_H$. Such correlation functions can be calculated order by order in perturbation theory in J_T up to $O(J_T)^4$ (see [23] for details), the results for $G(\omega)$ being identical for both ferromagnetic and antiferromagnetic systems.

We found that the spin resistance of AFs becomes *universal*,

$$R_M = \frac{h}{p(g\mu_{\rm B})^2}, \tag{13}$$

with $p = 2$ for a small magnetic dot (in the sense that the level spacing is always larger than the temperature) and $p = 1$ for a large quantum dot.[23] This implies that the resistance does not depend on material parameters of the magnetic dot. This result should be contrasted with the ferromagnetic case where the resistance is found to be generically non universal.[23] These predictions can be tested either in cold atomic system where spin chains Hamiltonians have been realized or in chains of adatoms adsorbed on an insulating substrate. We refer the reader to [23] for a detailed discussion of possible experimental realizations.

D. Rectification Effects and Magnon Transistor

Focusing again on both ferromagnetic and antiferromagnetic nonitinerant spin chains adiabatically connected to two spin reservoirs[21], we[26] have studied rectification effects. Using spin-wave formalism (i.e., Holstein-Primakoff transformation[11,12]) and the Landauer-Büttiker approach[62,80,102,103], it has been found in Ref. [26] that a spin anisotropy combined with an offset magnetic field is the crucial ingredient to achieve a nonzero rectification effect of spin currents in FMs. However, for AFs, a uniform anisotropy is not sufficient to achieve a sizable current rectification. Using Jordan-Wigner transformation (with a bosonization procedure) and TLL formalism[16,17,82–85], we have studied the scaling behavior of the antiferrromagnetic spin chain; the renormalization-group analysis[82] has shown that a spatially varying anisotropy, attained by a site impurity, instead realizes a sizable rectification effect. On top of this, using similar approach with the help of Schwinger-Keldysh formalism[104–112], we[27] have studied frequency-dependent spin transport and proposed a system that behaves as a *capacitor* for the spin degree of freedom; an anisotropy in the exchange interaction plays the key role in such a spin capacitor.

Finally, within a sequential tunneling approach for the describing the spin transport, we[24] have proposed an ultrafast magnon transistor at room temperature and a way to combine three magnon transistors to form a purely magnetic NAND gate[113] in Ref. 24 (see also Ref. 79). Focusing on transport of magnons and spinons through a triangular molecular magnet[114–118], it has been shown that electromagnetically changing the state of the molecular magnet, the magnitude of the spin current can be efficiently controlled.

III. MAGNON HALL EFFECTS IN AHARONOV-CASHER PHASE

Since magnons are magnetic dipoles $\mu_{\rm m} = -g\mu_{\rm B}\mathbf{e}_z$ a moving magnon in an electric field $\mathbf{E}$ acquires an Aharonov-Casher (A-C) phase θ_{ij} (Table II). In a two-dimensional Heisenberg FM, this motion is described by a spin (pointing along z) 'hopping' from site $\mathbf{x}_i$ to a neighboring site $\mathbf{x}_j$ and thereby picking up a Peierls phase factor $e^{-i\theta_{ij}}$ with A-C phase $\theta_{ij} \equiv [g\mu_{\rm B}/(\hbar c^2)]\int_{\mathbf{x}_i}^{\mathbf{x}_j} d\mathbf{x}\cdot(\mathbf{E}\times\mathbf{e}_z)$, where the integration runs along the straight line connecting the two neighboring lattice sites $\mathbf{x}_i$ and $\mathbf{x}_j$.[21] The corresponding Hamiltonian is given by[21] ($J < 0$)

$$\begin{aligned} H_2 &= \frac{J}{2}\sum_{\langle i,j\rangle}[S_i^+ S_j^- {\rm e}^{-i\theta_{ij}} + S_i^- S_j^+ {\rm e}^{i\theta_{ij}} + 2S_i^z S_j^z] \\ &+ g\mu_{\rm B}\sum_i B_i S_i^z, \end{aligned} \tag{14}$$

where the raising (lowering) operators $S_i^\pm = S_i^x \pm iS_i^y$ effectively describe the hopping of the spin component S_i^z. The Holstein-Primakoff transformation[12] maps spins into the magnon degrees of freedom and this Hamiltonian into the single magnon Hamiltonian h_2 in the presence of an effective electric 'vector potential' $\mathbf{A}_{\rm m} \equiv \mathbf{E}\times\mu_{\rm m}$,[21]

$$h_2 = \frac{\mid J \mid Sa^2}{\hbar^2}(\mathbf{p} - g\mu_{\rm B}\mathbf{E}\times\mathbf{e}_z/c^2)^2 + g\mu_{\rm B}B, \tag{15}$$

where a is the lattice constant. Then the mass of a magnon m is defined by $1/m \equiv 2 \mid J \mid Sa^2/\hbar^2$. The Heisenberg equation of motion, $m\ddot{\mathbf{x}} = i^2[h_2,[h_2,\mathbf{x}]] \equiv \mathbf{F}$, provides the force acting on a magnon,

$$\mathbf{F} = -g\mu_{\rm B}\nabla[B - (\mathbf{v}\times\mathbf{E})\cdot\mathbf{e}_z/c^2]. \tag{16}$$

This means that driven by a magnetic field gradient ∇B, magnons in an inhomogeneous electric field $\mathbf{E}(\mathbf{x})$ experience a force $\mathbf{F}$ analogous to the Lorentz force, which leads to phenomena analogous to classical Hall effects[21]. Thus the A-C effect gives a handle[28] to electromagnetically control magnon transport (see also Sec. IV C). Recently,

such an effect on magnons has been experimentally observed in Ref. [92] and magnonic Snell's law at interfaces, implying specular (elastic) reflection at the boundary to vacuum, has been experimentally established in Ref. [47]. Therefore, this analogy leads to the whole phenomenology of Hall effects such as the magnonic 'quantum' Hall effect[31,119,120], the thermal Hall effect in skyrmion lattices[25], the Hall effect in frustrated magnets[121], and the magnonic topological insulators[94,95,122–129] and their associated topologically protected edge states.

IV. MAGNON TRANSPORT IN INSULATING BULK MAGNETS

In 2010, Kajiwara *et al.*[63] experimentally demonstrated that it is possible to electrically create and readout a spin-wave spin current in the magnetic insulator $Y_3Fe_5O_{12}$ (YIG) by using both inverse[43] and spin Hall effects in Pt/YIG/Pt system. The weak spin damping of YIG enables the spin-wave spin current to carry spin-information over distances of several millimeters, much further than what is typically possible when using spin-polarized conduction electrons in metals.

A. Fundamentals of Magnon Physics

Thus, spin-waves (i.e., magnons[11,12]) play an essential role for magnetic currents in three-dimensional insulating magnets. Note that these systems are completely free from the restriction by the Mermin-Wagner theorem[13–15]; the spontaneous symmetry breaking in three dimensions is possible even in the thermodynamics limit. To reveal the transport properties of such low-energy magnetic modes is the main aim of this section.

To this end, we here (Sec. IV A) quickly review fundamentals[5–7,130–136] of spin waves and summarize the properties inherent to Bose particles (*e.g.*, magnons).

1. *Holstein-Primakoff Transformation*

As shown in Fig. 1, the low-energy physics is characterized by the collective spin mode (i.e., a gapless magnetic excitation), the spin wave, and the quantum description may be identified with magnons (Fig. 4). Assuming magnetically ordered states at zero temperature, spin degrees of freedom can be mapped into the magnon ones by the Holstein-Primakoff transformation[11,12]; focusing on the zero-mode (i.e., a single mode) just for simplicity, it becomes

$$S^+ = \sqrt{2S}\Big(1-\frac{a^\dagger a}{2S}\Big)^{1/2} a = (S^-)^\dagger, \tag{17a}$$

$$S^z = S - a^\dagger a, \tag{17b}$$

where S is the spin length ($S = \mathbb{N}_+/2 \gg 1$ with $\mathbb{N}_+ \equiv \{1,2,\cdots\}$) and the magnon annihilation (creation)

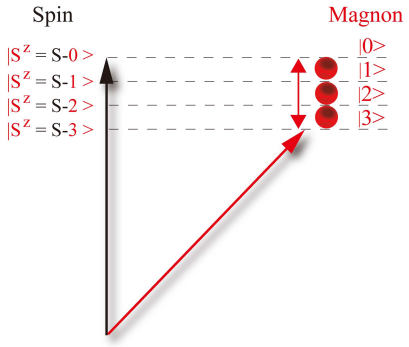

FIG. 4: (Color online) Schematic representation of the correspondence between spin and magnon degrees of freedom in the Holstein-Primakoff transformation. The magnitude of the deviation or the excitation from the ferromagnetically ordered state $|\, S^z = S\rangle$ at zero temperature is represented by the number of magnons. Magnons are absent in the spin polarized state $|\, S^z = S\rangle$.

operator $a^{(\dagger)}$ satisfies the bosonic commutation relation

$$[a, a^\dagger] = 1. \tag{18}$$

The number operator is given by $a^\dagger a$ and the eigenstate of the number operator, $|\, n\rangle$ with $n \in \mathbb{N}_0$ and $\mathbb{N}_0 \equiv \{0,1,2,\cdots\}$, satisfies

$$a\,|\,0\rangle = 0, \tag{19a}$$

$$a^\dagger a\,|\,n\rangle = n\,|\,n\rangle, \tag{19b}$$

$$a\,|\,n\rangle = \sqrt{n}\,|\,n-1\rangle, \tag{19c}$$

$$a^\dagger\,|\,n\rangle = \sqrt{n+1}\,|\,n+1\rangle, \tag{19d}$$

$$\langle n\,|\,a\,|\,n\rangle = 0. \tag{19e}$$

Note that it is not the eigenstate of the operators $a^{(\dagger)}$ [Eqs. (19c) and (19d)].

2. *Magnonic Coherent State*

The way of description changes when magnons are in condensation. Bosons are free from the Pauli principle and such a bosonic nature enables magnons to condensate[137]. Once magnons are in a condensate, they form a macroscopic coherent state and can be identified with a semiclassical object (see also Sec. VI A); the magnon *coherent state* $|\, \lambda\rangle$ can be characterized by the eigenstate of the annihilation operator a as

$$a\,|\,\lambda\rangle = \lambda\,|\,\lambda\rangle, \tag{20a}$$

$$\lambda \in \mathbb{C}, \tag{20b}$$

which means

$$\langle\lambda\,|\,a\,|\,\lambda\rangle \neq 0. \tag{21}$$

This is in sharp contrast to Eq. (19e). Thus, the expectation value of the operator a works[138] as a macroscopic

condensate order parameter and characterizes magnon condensation. Using it, we classify magnon states and reveal the resulting transport properties in Sec. IV C. As to the stability of the coherent state $|\ \lambda\rangle$ for the time evolution and the effects of magnon-magnon interactions on the coherent state, see Refs. [133–136].

B. Wiedemann-Franz Law for Magnon Transport

1. *Wiedemann-Franz Law*

In 1853, Wiedemann and Franz[71] experimentally established that at sufficiently low temperatures, the ratio between the electric and thermal conductances σ and K_e of free electrons, respectively, approximately reduces to the same value for different metals. In 1872, Lorenz discovered that the ratio becomes proportional to temperatures and now[62,139], the Wiedemann-Franz (WF) law is summarized as

$$\frac{K_e}{\sigma} \overset{\rightarrow}{=} \mathcal{L}T, \tag{22}$$

where the Lorenz number is defined by

$$\mathcal{L} \equiv \frac{\pi^2}{3}\left(\frac{k_{\rm B}}{e}\right)^2. \tag{23}$$

This is a fundamental hallmark that characterizes the universal thermoelectric properties of electron transport; the Lorenz number is independent of any material parameters. Note that since electrons are fermions (Table III), the WF law for electron transport can be characterized[139] only by diagonal transport coefficients L_e^{11} and L_e^{22} at low temperatures $T \ll \epsilon_{\rm F}/k_{\rm B}$ ($\sim 10^4$ K for a typical metal such as gold or copper), *i.e.*,

$$\frac{K_e}{\sigma} \approx \frac{L_e^{22} + \mathcal{O}\big((k_{\rm B}T/\epsilon_{\rm F})^2\big)}{L_e^{11}}, \tag{24}$$

where $\epsilon_{\rm F}$ is the Fermi energy and L_e^{ij} $(i,j=1,2)$ denotes the Onsager coefficient of electron transport that characterizes the response to driving forces (*e.g.*, electric field and gradients of chemical potential and temperature; see Ref. [139] for details).

On the other hand (Table III), magnons are bosons, without Pauli principle and thus without Fermi surface which defines the Fermi energy. It is well-known that the quantum-statistical properties of bosons and fermions show in general an entirely different dependence on system parameters, most notably on temperature; as an example, at low temperatures below Fermi and Debye temperatures, the specific heat C_V at constant volume of metals is given by[62] $C_V = \mathcal{C}_{\rm el}T + \mathcal{C}_{\rm ph}T^3$, where electrons (i.e., fermions) contribute to $\mathcal{C}_{\rm el}T$, while phonons (i.e., bosons) to $\mathcal{C}_{\rm ph}T^3$ with a constant $\mathcal{C}_{\rm el(ph)}$ that depends on material properties. Taking this into account, a fundamental question arises: can such a linear-in-T behavior [Eq. (22)] also arise for magnons? The answer is positive as we discuss next.

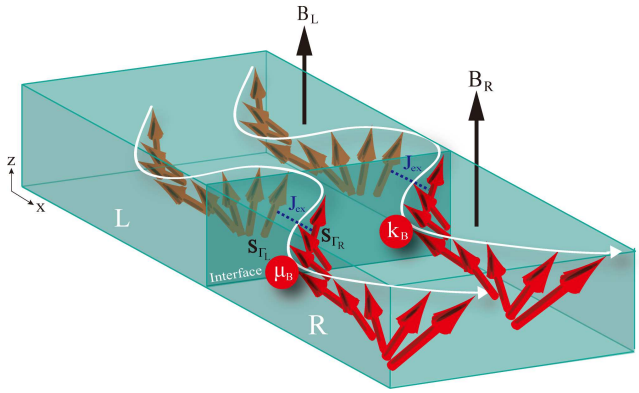

FIG. 5: (Color online) Schematic representation of a three-dimensional ferromagnetic insulating junction. The time reversal symmetry is broken by the ferromagnetic order and the magnetic field along the z-axis denoted by $B_{\rm L(R)}$. The boundary spins $\mathbf{S}_{\Gamma_{\rm L(R)}}$ are relevant to the magnon transport and they are weakly exchange-coupled with the strength $J_{\rm ex}$. Reprinted with permission from Ref. [30].

2. *Onsager Matrix of Magnon*

To this end, we[30] considered a magnetic junction formed by two ferromagnetic insulators (FI), as illustrated in Fig. 5, and investigated the transport of magnons. Focusing on thermally-induced magnons (i.e., noncondensed magnons; see Table IV), we found universal thermomagnetic properties of magnon transport.

Due to a finite overlap of the wave functions of the boundary spins, denoted as $\mathbf{S}_{\Gamma_{\rm L}}$ and $\mathbf{S}_{\Gamma_{\rm R}}$ in the left and right FI, respectively (see Fig. 5), there exists in general a finite exchange interaction described by the Hamiltonian

$$\mathcal{H}_{\rm ex} = -J_{\rm ex} \sum_{\langle \Gamma_{\rm L}\Gamma_{\rm R}\rangle} \mathbf{S}_{\Gamma_{\rm L}} \cdot \mathbf{S}_{\Gamma_{\rm R}}, \tag{25}$$

where $J_{\rm ex} > 0$ denotes the magnitude of the exchange interaction, weakly coupling the two FIs. Assuming large spins $S \gg 1$ and using the linearized Holstein-Primakoff expansion[12] $S^+ \approx \sqrt{2S}a$, the tunneling Hamiltonian can be written by magnon degrees of freedom

$$\mathcal{H}_{\rm ex}^{\rm tun} = -J_{\rm ex}S \sum_{\mathbf{k}_\perp} \sum_{k_x,k_x'} a_{\Gamma_{\rm L},\mathbf{k}} a^\dagger_{\Gamma_{\rm R},\mathbf{k}'} + {\rm H.c.}, \tag{26}$$

where $\mathbf{k} = (k_x, k_y, k_z)$, $\mathbf{k}' = (k_x', k_y, k_z)$, $\mathbf{k}_\perp = (0, k_y, k_z)$, and the bosonic operator $a^\dagger_{\Gamma_{\rm R/L}}$ $(a_{\Gamma_{\rm R/L}})$ creates (annihilates) a boundary magnon at the right/left FI. The k_x-momentum of magnons is not conserved at the sharp junction interface, whereas the perpendicular momentum $\mathbf{k}_\perp$ is conserved. We microscopically confirmed that the thermomagnetic properties of magnon transport in the junction qualitatively remain valid even when $k_x = k_x'$ in a model; the properties are robust against the microscopic details of the junction.

The tunneling Hamiltonian $\mathcal{H}_{\rm ex}^{\rm tun}$ thus gives the time-evolution of the magnon number operators in both FIs and generates the magnetic and heat currents. The temperature of the left (right) FI is $T_{\rm L(R)}$ and the magnetic field for magnons in the left (right) FI along the z-axis is $B_{\rm L(R)}$ with redefining $B_{\rm L} \equiv B$ and $T_{\rm L} \equiv T$ for convenience. The magnetic field and temperature differences are then defined by $\Delta B \equiv B_{\rm L} - B_{\rm R}$ and $\Delta T \equiv T_{\rm L} - T_{\rm R}$, respectively, and they generate the magnetic and heat (i.e., energy) currents[131,139] $\mathcal{I}_{\rm m}$ and $\mathcal{I}_Q$

$$\mathcal{I}_{\rm m} = -i(J_{\rm ex}S/\hbar)\sum_{\mathbf{k},\mathbf{k}'} g\mu_{\rm B} a_{\Gamma_{\rm L},\mathbf{k}} a^\dagger_{\Gamma_{\rm R},\mathbf{k}'} + {\rm H.c.}, \quad (27a)$$

$$\mathcal{I}_Q = -i(J_{\rm ex}S/\hbar)\sum_{\mathbf{k},\mathbf{k}'} \omega^{\rm L}_k a_{\Gamma_{\rm L},\mathbf{k}} a^\dagger_{\Gamma_{\rm R},\mathbf{k}'} + {\rm H.c.}, \quad (27b)$$

where $\omega^{\rm L}_k$ is the magnon dispersion relation in the left FI (see Ref. [30] for the detailed expression). The currents flow from the right FI to the left one when the sign of the currents is positive. Within the linear response regime, each Onsager coefficient L^{ij} $(i,j=1,2)$ is defined by

$$\begin{pmatrix} \langle \mathcal{I}_{\rm m} \rangle \\ \langle \mathcal{I}_Q \rangle \end{pmatrix} = \begin{pmatrix} L^{11} & L^{12} \\ L^{21} & L^{22} \end{pmatrix} \begin{pmatrix} \Delta B \\ -\Delta T \end{pmatrix}, \quad (28)$$

and it is evaluated by a straightforward perturbative calculation up to $\mathcal{O}(J_{\rm ex}^2)$ in $J_{\rm ex}$ based on the Schwinger-Keldysh formalism[104–112,140]. See Ref. [30] for detailed expressions of the Onsager coefficients, which depend on material parameters.

Both currents arise from terms of order $\mathcal{O}(J_{\rm ex}^2)$. Therefore, even when an electric field is applied to the interface, the resulting A-C phase cannot play any significant role in the transport of such noncondensed magnons. Moreover, even when a magnetic field difference $\Delta B \neq 0$ is generated, the noncondensed magnon current becomes essentially a dc one (Table IV). These are in sharp contrast to the condensed magnon current[28], which arises from the $\mathcal{O}(J_{\rm ex})$-term and can become an ac current (see Sec. IV C).

3. Magnon Seebeck and Peltier Coefficients

The time reversal symmetry is broken by the ferromagnetic order and the magnetic field, and therefore the Onsager reciprocal relation[141–143] could in principle be violated. Still, we microscopically found that the relation is satisfied (see Sec. IV B 7 for details)

$$L^{21} = T \cdot L^{12}. \quad (29)$$

This provides the Thomson relation (i.e., the Kelvin-Onsager relation[36])

$$\Pi = T\mathcal{S}, \quad (30)$$

where $\mathcal{S} \equiv L^{12}/L^{11}$ is the magnon Seebeck coefficient and $\Pi \equiv L^{21}/L^{11}$ is the magnon Peltier coefficient. At low temperatures, $\hbar/(2\tau) \ll k_{\rm B}T \ll g\mu_{\rm B}B$ with a phenomenologically introduced lifetime τ of magnons mainly due to nonmagnetic impurity scatterings, the coefficients reduce to (Fig. 6)

$$\mathcal{S} \overset{\rightrightarrows}{=} \frac{B}{T}, \qquad \Pi \overset{\rightrightarrows}{=} B. \quad (31)$$

The magnon Seebeck and Peltier coefficients thus become *universal* at low temperatures; including the g-factor, they are completely independent of any material parameters and are solely determined by the applied magnetic field and temperature.

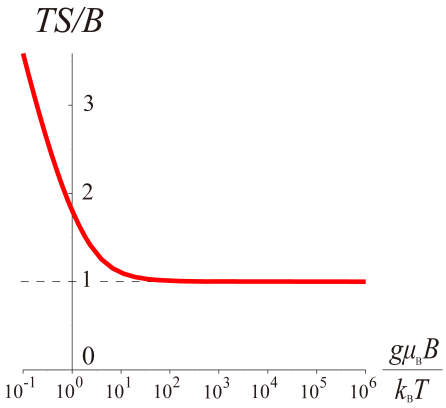

FIG. 6: (Color online) Plots of magnon Seebeck coefficient $\mathcal{S}$ as function of $g\mu_{\rm B}B/(k_{\rm B}T)$. At low temperatures $g\mu_{\rm B}B/(k_{\rm B}T) = \mathcal{O}(10^2)$, the rescaled coefficient $T\mathcal{S}/B$ approaches unity asymptotically and realizes the universal relation. Reprinted with permission from Ref. [30].

4. Thermal Conductance for Magnon Transport

The number of magnons increases when temperature becomes higher and magnetic fields weaker. Under the condition $\Delta T = 0$, the magnetic conductance G is defined by

$$\langle \mathcal{I}_{\rm m} \rangle \equiv G \cdot \Delta B, \quad (32)$$

which results in [Eq. (28)]

$$G = L^{11}. \quad (33)$$

The thermal conductance K is defined by[131,139]

$$\langle \mathcal{I}_Q \rangle \equiv -K \cdot \Delta T \quad \text{with} \quad \langle \mathcal{I}_{\rm m} \rangle = 0, \quad (34)$$

which can be understood as follows[144]; the applied temperature difference produces a magnon current and consequently a magnetization difference[145–147] that induces a counter current. Thus, the system reaches a new quasi-equilibrium steady state where magnon currents no longer flow. Since the condition for such quasi-equilibrium state $\langle \mathcal{I}_{\rm m} \rangle = 0$ results in a magnetization

TABLE III: Thermomagnetics of magnon transport. The time reversal symmetry is broken by the ferromagnetic order and the magnetic field, but the Onsager reciprocal relation is still satisfied. The Onsager relation ensures the Thomson relation, and vice versa. The magnon Seebeck and Peltier coefficients become universal at low temperatures $\hbar/(2\tau) \ll k_{\rm B}T \ll g\mu_{\rm B}B$ in the sense that including the g-factor, they are completely independent of any material parameters and are solely determined by the applied magnetic field and temperature. The WF law for electron transport is characterized[62,139] only by diagonal elements L_e^{11} and L_e^{22} due to the relatively large Fermi energy $\mathcal{O}\big((k_{\rm B}T/\epsilon_{\rm F})^2\big)$, while off-diagonal elements L^{21} and L^{12} are essential to the thermal conductance and the WF law for magnon transport since magnons are bosons. Still, the T-linear behavior holds in the same way for magnons despite the difference of quantum-statistical properties; the role of the charge e is played by $g\mu_{\rm B}$ and the magnetic Lorenz number is independent of any material parameters except the g-factor which is material specific.

	Electron	Magnon
Statistics	Fermi-Dirac	Bose-Einstein
Electric and magnetic conductance	$\sigma \equiv L_e^{11}$,	$G \equiv L^{11}$
Thermal conductance	$K_e \approx L_e^{22} + \mathcal{O}\big((k_{\rm B}T/\epsilon_{\rm F})^2\big)$,	$K \equiv L^{22} - L^{21}L^{12}/L^{11}$
WF law (low temperature)	$K_e/\sigma \approx [L_e^{22} + \mathcal{O}\big((k_{\rm B}T/\epsilon_{\rm F})^2\big)]/L_e^{11} \overset{\rightarrow}{=} \mathcal{L}T$,	$K/G \equiv (L^{22} - L^{21}L^{12}/L^{11})/L^{11} \overset{\rightarrow}{=} \mathcal{L}_{\rm m}T$
Lorenz number	$\mathcal{L} = \frac{\pi^2}{3}\left(\frac{k_{\rm B}}{e}\right)^2$	$\mathcal{L}_{\rm m} = \left(\frac{k_{\rm B}}{g\mu_{\rm B}}\right)^2$
Seebeck ($\mathcal{S}$) and Peltier (Π) coefficients	$\mathcal{S} \equiv L_e^{12}/L_e^{11}$, $\Pi \equiv L_e^{21}/L_e^{11}$	$\mathcal{S} \overset{\rightarrow}{=} \frac{B}{T}$, $\Pi \overset{\rightarrow}{=} B$
Onsager relation	$L_e^{21} = T \cdot L_e^{12}$	$L^{21} = T \cdot L^{12}$
Thomson relation	$\Pi = T\mathcal{S}$	$\Pi = T\mathcal{S}$

difference $\triangle B^* = (L^{12}/L^{11})\Delta T$ that gives the counter current, the thermal conductance is given by [Eq. (28)]

$$K = L^{22} - \frac{L^{21}L^{12}}{L^{11}}. \tag{35}$$

Note that in sharp contrast to charge transport [Eq. (24)], off-diagonal elements L^{21} and L^{12} which correspond to the counter current play a key role in the thermal conductance for magnon transport (see Table III) since magnons are bosons and thus L^{21} and L^{12} are not suppressed by a large Fermi energy. The information from all elements of the Onsager matrix [Eq. (28)] is essential for the thermal conductance of bosons.

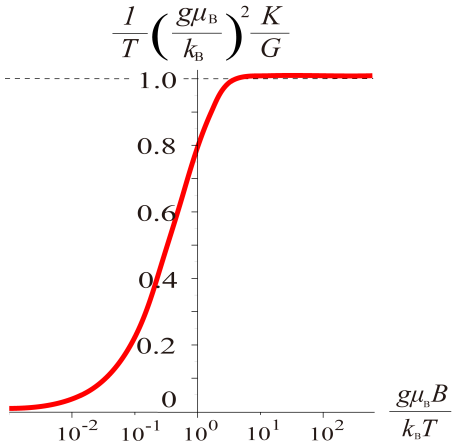

FIG. 7: (Color online) Plots of the ratio $(g\mu_{\rm B}/k_{\rm B})^2[K/(GT)]$ as function of $g\mu_{\rm B}B/(k_{\rm B}T)$. The ratio reaches the constant '1' and the WF law for magnon transport is realized at low temperatures $g\mu_{\rm B}B/(k_{\rm B}T) = \mathcal{O}(10)$; otherwise, the linear-in-T behavior breaks down. Reprinted with permission from Ref. [30].

Microscopic calculation shows that at low temperatures $\hbar/(2\tau) \ll k_{\rm B}T \ll g\mu_{\rm B}B$, the ratio becomes linear in temperature (Fig. 7)

$$\frac{K}{G} \overset{\rightarrow}{=} \left(\frac{k_{\rm B}}{g\mu_{\rm B}}\right)^2 T. \tag{36}$$

Therefore, in analogy to charge transport in metals[62,71,139], we refer to this behavior as the *Wiedemann-Franz law for magnon transport*. The constant $\mathcal{L}_{\rm m}$ analogous to the Lorenz number is given by

$$\mathcal{L}_{\rm m} \equiv \left(\frac{k_{\rm B}}{g\mu_{\rm B}}\right)^2, \tag{37}$$

where the role of the charge e is played by $g\mu_{\rm B}$. Therefore we refer to this constant as the *magnetic Lorenz number*. The magnetic Lorenz number is independent of any material parameters except the g-factor which is material specific. Interestingly, the T-linear behavior holds in the same way for magnons despite the fundamental difference between the quantum-statistical properties of bosons and fermions. The thermomagnetic properties are summarized in Table III.

One might suspect that such a T-linear behavior can be qualitatively expected from the unit conversion. However, without the microscopic calculations, one can not eliminate the possibility that the ratio becomes $K/G \propto T[k_{\rm B}T/(g\mu_{\rm B}B)]^{m-1} \propto T^m$ with *msomeinteger* even within linear response theory [Eq. (28)] since the driving force for magnon transport is not B but ΔB; consequently, each Onsager coefficient is characterized by an expansion of the dimensionless quantity $g\mu_{\rm B}B/(k_{\rm B}T)$. See Fig. 7. Indeed, if one (wrongly) omits the off-diagonal elements L^{12} and L^{21}, the ratio K/G is not proportional to temperature and reduces to a wrong result. Thus the linear-in-T behavior can be traced back to the Onsager relation between the off-diagonal elements [Eq. (29)]. The magnon WF law becomes violated when the Onsager relation is broken.

5. Magnon-magnon interaction

We microscopically found that the anisotropy induced magnon-magnon interaction $J_{\rm m}$ provides a 'nonlinearity' in terms of the perturbative terms and violates the Onsager relation (see Ref. [30] for details); it gives contributions δL^{11} and δL^{21}, and the Onsager matrix in Eq. (28) is replaced by

$$\begin{pmatrix} L^{11} & L^{12} \\ L^{21} & L^{22} \end{pmatrix} \mapsto \begin{pmatrix} L^{11}+\delta L^{11} & L^{12} \\ L^{21}+\delta L^{21} & L^{22} \end{pmatrix}, \tag{38}$$

where $\delta L^{11} = \mathcal{O}(J_{\rm ex}^2 J_{\rm m})$ and $\delta L^{21} = \mathcal{O}(J_{\rm ex}^2 J_{\rm m})$, while $L^{11} = \mathcal{O}(J_{\rm ex}^2 J_{\rm m}^0)$ and $L^{21} = \mathcal{O}(J_{\rm ex}^2 J_{\rm m}^0)$. This can be understood as follows (see Appendix D in Ref. [30] for details); the magnon-magnon interaction acts as an effective magnetic field and in an external magnetic field difference ΔB, the total magnetic field difference $\Delta B_{\rm tot}$ becomes $\Delta B_{\rm tot} = (1+b_{\rm m})\Delta B$ with $b_{\rm m} = \mathcal{O}(J_{\rm m})$. The term $b_{\rm m}$ gives $\delta L^{11} = \mathcal{O}(J_{\rm m})$ and $\delta L^{21} = \mathcal{O}(J_{\rm m})$, and the magnitude of the effective magnetic field difference can be estimated by $b_{\rm m} \sim \delta L^{21}/L^{21}$. The Onsager relation is thus violated due to the nonlinearity caused by the anisotropy induced magnon-magnon interaction. However, at low temperatures, where the WF law and the universality of Seebeck and Peltier coefficients hold (*e.g.*, $T = 0.7$K and $B = 5$T), these deviations become negligible $|\delta L^{ij}/L^{ij}| \ll 1$ and consequently, the Onsager relation and the WF law approximately hold. At such low temperatures $T \sim 10^{-1}$K, phonon contributions[148] are negligible[66].

6. Universality

So far we have assumed bulk FIs where magnetic dipole-dipole interactions are negligible[149]. Such dipolar effects, however, become important in thin films, resulting in a modified dispersion for magnons where the lowest energy mode becomes $k = k_{\rm m} \sim 10^4$/cm for YIG thin films[32,150,151]; the magnitude of $k_{\rm m}$ depends on the width of YIG thin films. We microscopically confirmed[30] that the WF law (i.e., the T-linear behavior) still remains valid in this case too, underlining the universality of this law. See Ref. [30] for details.

We mention that in sharp contrast to the three-dimensional insulating ferromagnets, quasiparticle pictures (*e.g.,* magnons) become broken down due to strong quantum fluctuations in the one-dimensional integrable spin-1/2 XXZ chain. Still, the linear-in-T behavior is satisfied[48] at low temperatures; it does not depend on the dimensionality. Therefore the T-linear behavior may be identified with the universal thermomagnetic properties of spin transport. See Refs. [50–54] for the progress[55] on the WF law for non-Fermi liquids.

7. Remark: Onsager-Thomson Relation

Our microscopic calculation (see Ref. [30] for details) showed that magnetic and heat currents [Eqs. (27a) and (27b)] are characterized by the difference of Bose-distribution functions $n_{\rm B}(\omega)$. Expanding in powers of $|\Delta T| \ll T$ and $|\Delta B| \ll B$ within the linear response regime, the difference becomes [$\beta \equiv 1/(k_{\rm B}T)$]

$$n_{\rm B}(\omega_{\mathbf{k}}^{\rm L}) - n_{\rm B}(\omega_{\mathbf{k}}^{\rm R}) \approx \begin{cases} -\beta \frac{g\mu_{\rm B} e^{\beta\omega_{\mathbf{k}}}}{(e^{\beta\omega_{\mathbf{k}}}-1)^2}\Delta B, & \text{for } \Delta T = 0, \\ \frac{\beta\omega_{\mathbf{k}}}{T}\frac{e^{\beta\omega_{\mathbf{k}}}}{(e^{\beta\omega_{\mathbf{k}}}-1)^2}\Delta T, & \text{for } \Delta B = 0, \end{cases} \tag{39}$$

which yields

$$\frac{[n_{\rm B}(\omega_{\mathbf{k}}^{\rm L}) - n_{\rm B}(\omega_{\mathbf{k}}^{\rm R})]\,|_{\Delta B=0}\,/\Delta T}{[n_{\rm B}(\omega_{\mathbf{k}}^{\rm L}) - n_{\rm B}(\omega_{\mathbf{k}}^{\rm R})]\,|_{\Delta T=0}\,/\Delta B} = -\frac{\omega_{\mathbf{k}}^{\rm L}}{g\mu_{\rm B}T}. \tag{40}$$

Eq. (40) is responsible for the Onsager-Thomson relations, given in Eqs. (29) and (30). Thus, we found that the magnetic and heat currents are characterized by the difference of the Bose-distribution functions, and the difference gives the linear responses [Eqs. (39) and (40)], and the Onsager-Thomson relations, Eqs. (29) and (30), hold accordingly.

Such results [*e.g.*, Eq. (39)] might be provided or expected also by the Landauer-Büttiker formalism[62,80,102,103]. However, the method is applicable only to noninteracting case, while the Schwinger-Keldysh formalism[104–112] enabled us to perturbatively evaluate the effect of the anisotropy induced magnon-magnon interaction.

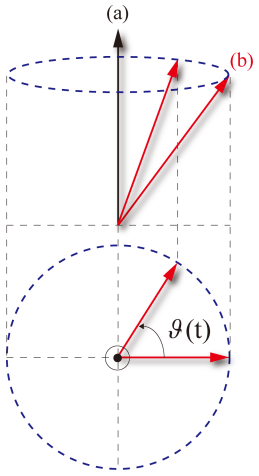

FIG. 8: (Color online) (a) A spin polarized state in the ground state, where magnons are absent. (b) A spin precession with the frequency $d\vartheta(t)/dt \neq 0$. In quasiequilibrium magnon condensation, all spins precess with the same finite frequency $d\vartheta(t)/dt$ and in terms of spin variables, such quasiequilibrium magnon condensation can be identified with a macroscopic coherent spin precession, see Fig. 10.

C. Magnon Josephson Effects

Next, focusing on magnons in quasiequilibrium[32,150–152] condensation, we investigate the transport properties and clarify differences from the noncondensed magnons.

1. *Quasiequilibrium Condensation of Excited Magnons*

In 2006, Demokritov *et al.*[32] experimentally realized *quasiequilibrium*[138,153–155] magnon condensates in YIG thin film by microwave pumping method at room temperature. Using Brillouin light scattering spectroscopy[156], the relation between microwave pumping and the resulting magnon condensate was investigated in detail by Serga *et al.*[150] and Calusen *et al.*[151]; magnetic dipole-dipole interactions become relevant in YIG thin film and the lowest energy mode of magnons becomes nonzero $k_{\rm m} \neq 0$ (*e.g.*[32,150,151], $k_{\rm m} \sim 10^4/{\rm cm}$), which plays the key role on the formation of quasiequilibrium magnon condensates. The applied microwave drives the system into a *nonequilibrium* steady state and continues to populate the zero-mode of magnons with breaking the $U(1)$-symmetry. After switching off the microwaves, the $U(1)$-symmetry is recovered and the number of magnons becomes conserved. Then toward the true lowest energy state $k_{\rm m} \neq 0$, the system undergoes a thermalization[151] (or relaxation[157–163]) process and thereby reaches a metastable[138,153–155] state where the pumped magnons form a *quasiequilibrium* magnon condensate[164]. The quasiequilibrium magnon condensate is not the ground state but a metastable[138,153–155] state that corresponds to a macroscopic coherent precession[165] in terms of spin variables which can last[32,150,151] for a few hundred nanoseconds.

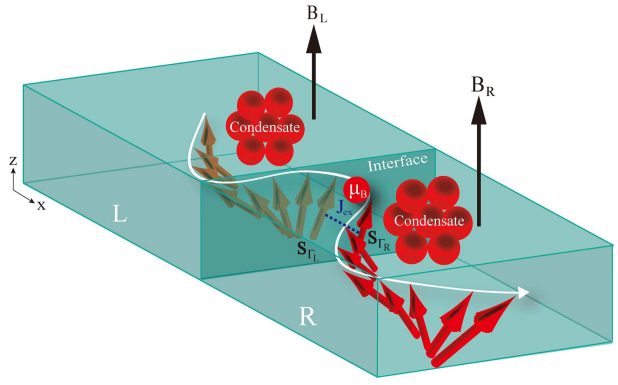

FIG. 9: (Color online) Schematic representation of a magnonic Josephson junction at zero temperature. See also Fig. 5. Reprinted with permission from Ref. [28].

From a theoretical viewpoint, in sharp contrast to noncondensed magnons, such quasiequilibrium condensed magnons are characterized by a macroscopic condensate order parameter commonly called the off-diagonal long-range order (ODLRO)[136,138,166]

$$\langle a(t)\rangle = \sqrt{N_{\rm cond.}}{\rm e}^{i\vartheta(t)}, \tag{41}$$

where $N_{\rm cond.} = \langle a(t)\rangle^* \langle a(t)\rangle$ is the number of condensed magnons and $\vartheta(t)$ denotes the phase (Fig. 8; we recall the linearized transformation[12] $S^+ \approx \sqrt{2S}a$). The ODLRO becomes zero when magnons are not in condensation. The quasiequilibrium magnon condensate is realized not in the ground state but in the metastable state, indicating that the phase becomes time-dependent,

$$\frac{d\vartheta(t)}{dt} \neq 0. \tag{42}$$

In such a quasiequilibrium condensate phase, all spins precess with the same finite frequency $d\vartheta(t)/dt$ and can be identified with a macroscopic coherent spin precession. See Figs. 8 and 10.

Note that throughout this paper, we use the terminology 'magnon coherent state' for the state which gives a nonzero value to the ODLRO $\langle a\rangle \neq 0$. In terms of the spin variables, $\langle a\rangle \equiv \sqrt{N_{\rm cond.}}{\rm e}^{i\vartheta} \neq 0$ means that all spins precess with the same frequency (i.e., *coherently*) and a constant phase difference, which we call macroscopic *coherent* spin precession; such coherent spin precession might be identified with a precession of a macroscopic spins and therefore, it could be treated *semiclassically* (see also Sec. VI A). See Refs. [133,134] for the time-evolution of coherent states.

2. *Magnon Josephson Equation*

The ODLRO is analogous to the order parameter for the conventional superconductors (Table V). Therefore in analogy to the superconductors, we[28] can discuss the condensed magnon transport in the magnetic insulating junction (Fig. 9) and found the Josephson effects.

Assuming $T_{\rm L} = T_{\rm R} = 0$, the quasiequilibrium magnon condensates in the junction are characterized by

$$\langle a_{\rm L(R)}(t)\rangle = \sqrt{n_{\rm L(R)}(t)}{\rm e}^{i\vartheta_{\rm L(R)}(t)}, \tag{43}$$

where the variable $n_{\rm L(R)}(t)$ represents the number density of condensed magnons in the left (right) FI and $\vartheta_{\rm L(R)}(t)$ denotes the phase (see Ref. [28] for the Gross-Pitaevskii Hamiltonian derived from the original spin Hamiltonian). The magnon population imbalance and the relative phase are defined by

$$z(t) \equiv [n_{\rm L}(t) - n_{\rm R}(t)]/n_{\rm T}, \tag{44a}$$
$$\theta(t) \equiv \vartheta_{\rm R}(t) - \vartheta_{\rm L}(t), \tag{44b}$$

where the constant $n_{\rm T} \equiv n_{\rm L}(t) + n_{\rm R}(t)$ denotes the total population in the junction. After switching off the microwaves, the $U(1)$-symmetry of the system is recovered and the number of condensed magnons may be assumed

TABLE IV: Properties of noncondensed magnons and those of magnons in quasiequilibrium condensation. They are distinguished by the ODLRO $\langle a\rangle$ associated with a macroscopic coherent state. Phases play the key role on the transport of magnons in quasiequilibrium condensation and a magnetic field difference $\Delta B \neq 0$ leads to ac Josephson currents, while dc currents when magnons are not in condensation. This is a good platform to experimentally observe condensed magnon currents. The quasiequilibrium magnon condensate is realized not in the ground state but in the metastable state, where all spins precess with the same frequency $d\vartheta(t)/(dt) \neq 0$ and can be identified with a macroscopic coherent spin precession. The number of magnons in quasiequilibrium condensation and the time-evolution can be experimentally[32,150,151] investigated by Brillouin light scattering spectroscopy[156], and at room temperature, the number density of noncondensed magnons is[32] much larger than that of such condensed magnons.

Noncondensed magnon (i.e., thermally-induced magnon[138,167])	Quasiequilibrium condensed magnon
$\langle a\rangle = 0$	$\langle a\rangle \neq 0$
Individual magnon	Macroscopic coherent magnon state
Incoherent spin precession	Macroscopic coherent spin precession
Fig. 10 (c)	Fig. 10 (a) and (b)
$\langle a^\dagger a\rangle \sim \int d\omega (e^{\beta\omega}-1)^{-1}$	$N_{\rm cond.} = \langle a(t)\rangle^* \langle a(t)\rangle$ with $\langle a(t)\rangle = \sqrt{N_{\rm cond.}} e^{i\vartheta(t)}$
Sum over various low-energy modes	A macroscopic number of magnons occupies a single state
Magnon current (i.e., spin-wave spin current[63])	Condensed magnon current[168]
Number density[32] at room temperature; 10^{21}-10^{23}cm^{-3}	Number density[32] at room temperature; 10^{18}-10^{19}cm^{-3}
A dc current $\mathcal{O}(J_{\rm ex}^2)$ by $\Delta B \neq 0$ in the junction (Fig. 5)	An ac current $\mathcal{O}(J_{\rm ex})$ by $\Delta B \neq 0$ in the junction (Fig. 5)
Voltage drop $V_{\rm m}$ in Fig. 14: $V_{\rm m}$ ∼mV	Voltage drop $V_{\rm m}$ in Fig. 14: $V_{\rm m}$ ∼nV

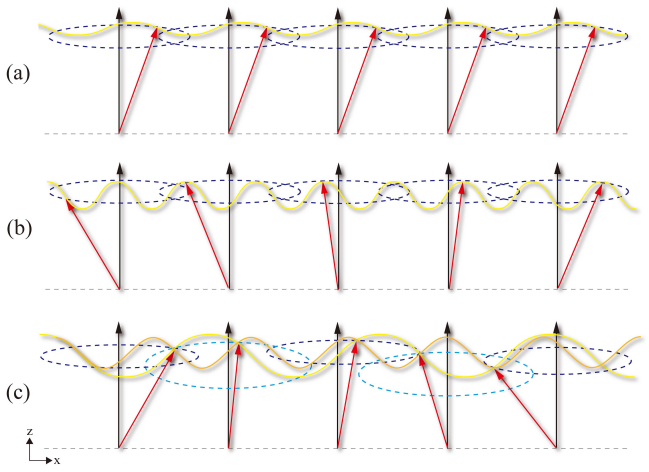

FIG. 10: (Color online) Schematic representations of (a) a macroscopic coherent spin precession, (b) a macroscopic coherent spin precession in A-C effects, and (c) an incoherent spin precession. The dashed blue lines represent a spin precession on a plane, and the frequency is different from the one in light blue. All spins precess with the same frequency (i.e., coherently) in (a) and (b), while not in (c). In terms of spin variables, quasiequilibrium magnon condensates[32,150,151] correspond to (a) and (b). Applying an external electric field $\mathbf{E} = E\mathbf{e}_y$ in (b) with a lattice constant a, the resulting A-C effects generate a constant phase difference $\theta_{\text{A-C}} = [g\mu_{\rm B}/(\hbar c^2)]Ea$ between the individual spins, but still they precess with the same frequency, which leads to a persistent current in a ring (Fig. 13).

to be conserved at zero temperature. An external electric field $\mathbf{E} = E\mathbf{e}_y$ is applied to the interface. Consequently, during the tunneling process, magnons acquire the A-C phase (Table II) and it is described by

$$\mathcal{H}_{\rm ex}^{\text{A-C}} = -J_{\rm ex}S \sum_{\langle \Gamma_{\rm L}\Gamma_{\rm R}\rangle} (a_{\Gamma_{\rm L}} a_{\Gamma_{\rm R}}^\dagger e^{-i\theta_{\text{A-C}}} + \text{h.c.}), \quad (45)$$

where $\theta_{\text{A-C}} = [g\mu_{\rm B}/(\hbar c^2)]E\Delta x$ for the geometry under consideration and now Δx is the distance between boundary spins. This A-C effect gives a handle to electromagnetically control magnon transport in the junction. Note that such an effect on magnons has been experimentally observed recently in Ref. [92]. In terms of the canonically conjugate variables $z(t)$ and $\theta(t)$, the condensed magnon transport in the junction is described by

$$\frac{dz}{d\mathcal{T}} = -\sqrt{1-z^2}\sin(\theta+\theta_{\text{A-C}}), \quad (46a)$$

$$\frac{d\theta}{d\mathcal{T}} = \Delta\mathcal{E} + \Lambda z + \frac{z}{\sqrt{1-z^2}}\cos(\theta+\theta_{\text{A-C}}), \quad (46b)$$

where

$$\mathcal{T} \equiv 2K_0 t/\hbar, \quad (47a)$$

$$\Delta\mathcal{E} = \frac{\mathcal{E}_{\rm L}-\mathcal{E}_{\rm R}}{2K_0} + \frac{U_{\rm L}-U_{\rm R}}{4K_0} n_{\rm T}, \quad (47b)$$

$$\Lambda = \frac{U_{\rm L}+U_{\rm R}}{4K_0} n_{\rm T}, \quad (47c)$$

with

$$\mathcal{E}_{\rm L(R)} = 4JS(1-\eta) + g\mu_{\rm B}B_{\rm L(R)}, \quad (48a)$$

$$U_{\rm L(R)} = -2J(1-\eta)a^3. \quad (48b)$$

The tunneling amplitude is defined by $K_0 \equiv J_{\rm ex}S$ and magnon-magnon interactions arise[29] from the spin anisotropy $0 < \eta \neq 1$ [Eq. (48b)] of the spin Hamiltonian $\mathcal{H}_{\rm H}$ for a single FI given by ($J < 0$) $\mathcal{H}_{\rm H} =$

$\sum_{\langle ij\rangle} \mathbf{S}_i \cdot \mathbf{J} \cdot \mathbf{S}_j - g\mu_{\rm B}\mathbf{B} \cdot \sum_i \mathbf{S}_i$, where $\mathbf{J}$ denotes a diagonal 3×3-matrix with $\mathrm{diag}(\mathbf{J}) = J\{1, 1, \eta\}$. Eqs. (46a) and (46b) are the magnon Josephson equations: Eq. (46a) describes the magnon Josephson current and Eq. (46b) the time-evolution of the relative phase, which mean that the phases $\vartheta_{\rm R}(t)$ and $\vartheta_{\rm L}(t)$ play the key role on magnon transport in quasiequilibrium condensation. The magnon Josephson current arises from terms of order $\mathcal{O}(J_{\rm ex})$, which is in sharp contrast to the noncondensed magnon current $\mathcal{O}(J_{\rm ex}^2)$ in the junction (see Tables IV and V). Thus the condensed magnon transport in the junction is described by the magnon Josephson equations. We note for condensed magnons, noncondensed magnons work as an effective magnetic field and such an effect can be taken into account in $B_{\rm L(R)}$ [Eq. (48a)].

Fig. 11 shows a numerical plot of ac Josephson effect and that of a macroscopic quantum self-trapping (MQST). The self-interaction $\Lambda \neq 0$ results from spin anisotropies $\eta \neq 1$ and characterizes the period of ac Josephson effects. A MQST occurs[169–172] when the value satisfies $\Lambda > \Lambda_{\rm c}$, where

$$\Lambda_{\rm c} = \frac{1 + \sqrt{1 - z(0)^2}\cos(\theta(0) + \theta_{\text{A-C}})}{z(0)^2/2}. \tag{49}$$

On the other hand, in the isotropic case $\eta = 1$ (i.e., $\Lambda = 0$), ac Josephson effects become characterized by the nonlinear effect $(z/\sqrt{1 - z^2})\cos(\theta + \theta_{\text{A-C}})$ in Eq. (46b). We numerically found that the period is determined by the nonlinear effect and little influenced by the magnetic field difference $\Delta\mathcal{E}$ since the maximum value of magnetic field gradient within experimental reach is estimated by $\partial B/(\partial x) \leq 1\mathrm{T/cm}$, which results in $\Delta\mathcal{E} \leq 1$. Even without any magnetic field differences, ac Josephson effects are generated by the nonlinear effect with an initial population imbalance $z(0) \neq 0$. The period $t_{\rm ac}$ is estimated by $t_{\rm ac} = 3\hbar/(J_{\rm ex}S)$, which becomes within experimental reach[173] $t_{\rm ac} = 10\mathrm{ns}$ when $J_{\rm ex} = 0.03\mu\mathrm{eV}$ and $S = 10$ as an example. Such a weak tunneling amplitude may be realized by inserting a thin nonmagnetic insulator (NI) between the FIs and realizing the multi-layered Josephson junction FI/NI/FI.

Fig. 12 shows numerical plots of a dc Josephson effect and a transition between the ac and dc Josephson effects. A dc Josephson effect is generated by a time-dependent magnetic field whose magnitude increases over time with a rate b_0 for a limited rescaled time $\mathcal{T}_0$;

$$\Delta\mathcal{E}(\mathcal{T}) = \frac{g\mu_{\rm B}}{2K_0}\left(B_{\rm L} - B_{\rm R}\right) = \begin{cases} -b_0\mathcal{T} & \text{for } \mathcal{T} \in (0, \mathcal{T}_0), \\ 0 & \text{otherwise.} \end{cases} \tag{50}$$

Assuming $\Lambda \gg 1$ and $|z| \ll 1$, the Josephson equations [Eqs. (46a) and (46b)] reduce to

$$\frac{dz}{d\mathcal{T}} \approx -\sin(\theta + \theta_{\text{A-C}}), \tag{51a}$$

$$\frac{d\theta}{d\mathcal{T}} \approx -b_0\mathcal{T} + \Lambda z. \tag{51b}$$

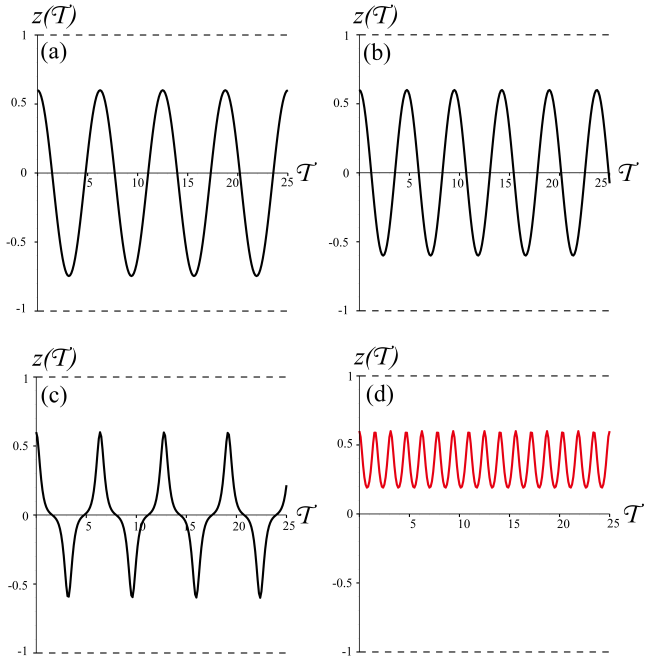

FIG. 11: (Color online) The ac Josephson effects: Plots of the population imbalance $z(\mathcal{T})$ as function of the rescaled time $\mathcal{T} = (2J_{\rm ex}S/\hbar)t$. The rescaled time $\mathcal{T} = 1$ corresponds to $t = 1$ ns for $J_{\rm ex} = 0.25$ μeV and $S = 2$. (a) $\Delta\mathcal{E} = 0.1$, $\Lambda = 0$, $\theta_{\text{A-C}} = 0$, $z(0) = 0.6$, and $\theta(0) = 0$. The period of an oscillation is $\mathcal{T} = 6$ ns. (b) - (d) $\Delta\mathcal{E} = \theta_{\text{A-C}} = 0$, $z(0) = 0.6$, and $\theta(0) = 0$, which give $\Lambda_{\rm c} = 10$. (b) $\Lambda = 1$, (c) $\Lambda = 9.99$, and (d) $\Lambda = 11$: The MQST occurs since $\Lambda > \Lambda_{\rm c}$. Reprinted with permission from Ref. [28].

The steady-state solution of dc effects for a finite time is given by

$$z(\mathcal{T}) = z_0\mathcal{T} \text{ and } \theta(\mathcal{T}) = -\arcsin(z_0) - \theta_{\text{A-C}}, \tag{52}$$

with $z_0 \equiv b_0/\Lambda$. Supposing $\theta(0) = 0$, we remark that unless $\theta_{\text{A-C}}$ is tuned to the value

$$\theta_{\text{A-C}} = -\arcsin(z_0), \tag{53}$$

a mismatch in $\theta(\mathcal{T})$ with the steady-state solution arises. This leads to a phenomenon that the value of z_0 for a transition between the ac and dc Josephson effects is reduced by a numerical factor ≈ 0.725. See Ref. [28] for details.

So far we have assumed bulk FIs where magnetic dipole-dipole interactions are negligible[149]. Such dipolar effects, however, become important in thin films, resulting in a modified dispersion for magnons where the lowest energy mode becomes $k = k_{\rm m} \sim 10^4/\mathrm{cm}$ for YIG thin films[32,150,151,163]; the magnitude of $k_{\rm m}$ depends on the width of YIG thin films. Still, we confirmed[174] that the magnon Josephson effects qualitatively remain valid; the contribution is added into $\mathcal{E}_{\rm L(R)}$ in Eq. (48a) and it is modified by $\mathcal{E}_{\rm L(R)} = 4JS(1 - \eta) + g\mu_{\rm B}B_{\rm L(R)} - JS(1 +$

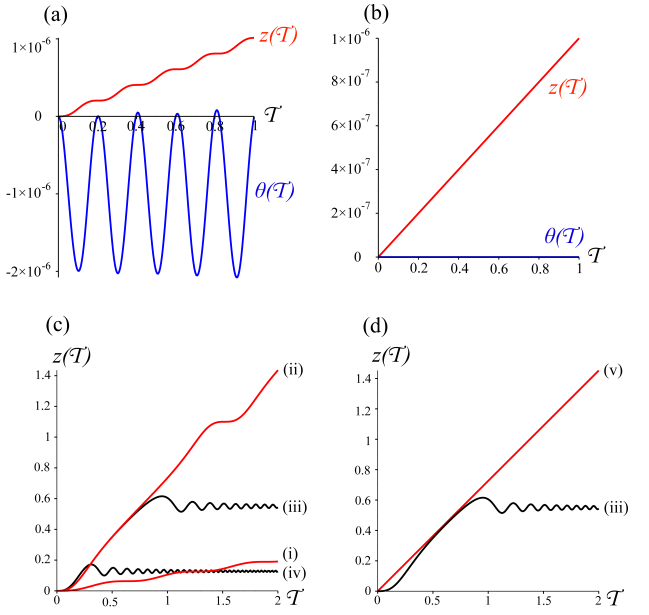

FIG. 12: (Color online) The dc Josephson effects: Plots of the population imbalance $z(\mathcal{T})$ and the relative phase $\theta(\mathcal{T})$ as function of the rescaled time $\mathcal{T}$. for (a) (b) $z_0 = 10^{-6}$, $\Lambda = 10^3 (\gg 1)$, and $z(0) = \theta(0) = 0$. (a) $\theta_{\text{A-C}} = 0$. (b) $\theta_{\text{A-C}} = -\arcsin(z_0) = -10^{-6}$. (c) The breakdown of the dc Josephson effect ($\theta_{\text{A-C}} = 0$) due to increase of b_0. The transition between the dc region [(i), (ii)] and the ac one [(iii), (iv)] takes place for $z_0 \approx 0.725$ due to the absence of the A-C phase. On the conditions $(z(0), \theta(0)) = (0, 0)$ and $\Lambda = 100$ ($\gg 1$), each $z_0 = b_0/\Lambda$ reads (i) 0.100, (ii) 0.724, (iii) 0.726, and (iv) 1.100. (d) Example of the recovery of the dc Josephson effect from the ac effect through the A-C phase in the region $z_0 \leq 1$ (i.e., $b_0 \leq \Lambda$). (iii) $\theta_{\text{A-C}} = 0$, (v) $\theta_{\text{A-C}} = -\arcsin(z_0)$. Reprinted with permission from Ref. [28].

$\eta)(ak_{\text{m}}^{\text{L(R)}})^2$, where $k_{\text{m}}^{\text{L(R)}}$ is the lowest energy mode in the left (right) FI.

Lastly, we remark that when $\theta_{\text{A-C}} = 0$ in Eqs. (46a) and (46b), the description mathematically reduces to the one for cold atoms[167,169–171,175], where the Josephson effects and the MQST have already been observed[172,176] experimentally. Similar equations for $\theta_{\text{A-C}} = 0$ have been proposed phenomenologically for ferromagnets[177] and for antiferromagnets[178]. It should be noted[179] that *Bose-Einstein condensation* of magnons and the resulting several phenomena (*e.g.*, Josephson effects) in Helium-3 have already been intensively investigated by Bunkov-Volovik[138], and the microscopic mechanisms are well understood both theoretically and experimentally. See Refs. [180,181] as an example and the review article [138] for details of their works on Helium-3.

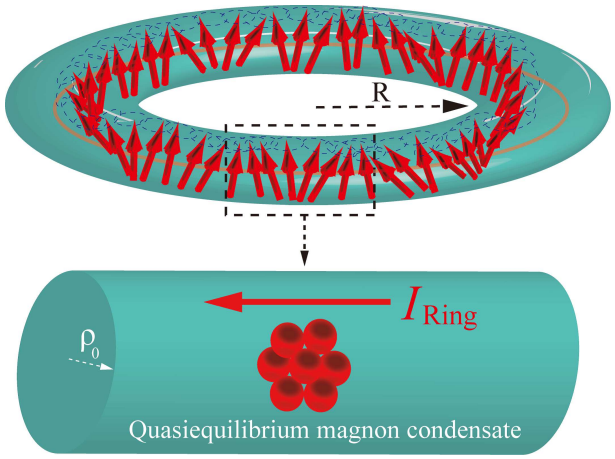

FIG. 13: (Color online) Schematic representation of a condensed magnon ring with the radius R and the enlarged view of the cylindrical wire that forms the ring. The radius of the wire is ρ_0. A-C effects generate phase differences between the individual spins, but still they precess with the same frequency (i.e., coherently) [Fig. 10 (b)]. Consequently, a condensed magnon current I_{Ring} flows 'persistently' in the ring as long as magnons are in quasiequilibrium condensation. Any persistent currents in the ground state are forbidden by Bloch theorem[183] and such a persistent current is possible since quasiequilibrium magnon condensates are not the ground state but a metastable state. The current is not steady when the quantization condition [Eq. (54)] is not satisfied. However, the non-steady variations of the current away from its nonequilibrium steady state are negligibly small. This setup was proposed in Ref. [28] and reprinted with permission.

D. Persistent Current and Quantization in Ring

In analogy to a superconducting ring[184,185] (see Table V), we introduce a condensed magnon ring as sketched in Fig. 13 and discuss the 'persistent' condensed magnon current by the A-C effect. Similar setup was proposed in Refs. [18,19,186,187].

Due to the single-valuedness of the wave function of condensed magnons (i.e., macroscopically precessing localized spins) around the ring, the electric flux ϕ is quantized as

$$\phi = p\phi_0 \quad \text{with} \quad p \in \mathbb{Z}, \tag{54}$$

where the integer p is the phase winding number of the closed path around the ring with

$$\theta_{\text{A-C}} = \frac{g\mu_{\text{B}}}{\hbar c^2} \oint_{\text{Ring}} \mathrm{d}\mathbf{l} \cdot (\mathbf{E} \times \mathbf{e}_z) \tag{55a}$$

$$\equiv 2\pi \frac{\phi}{\phi_0}, \tag{55b}$$

and the electric flux quantum[187]

$$\phi_0 \equiv hc^2/(g\mu_{\text{B}}). \tag{56}$$

TABLE V: Magnon analogues of the conventional superconductors characterized[166] by the order parameter for copper pairs, $\langle c_{\mathbf{k}\uparrow}c_{-\mathbf{k}\downarrow}\rangle$, where c is an annihilation operator for fermions. Josephson effects in junction of two bulk superconductors are characterized by the canonically conjugate variables; the number imbalance $\Delta\mathcal{N}$ and the relative phase $\Delta\varphi$. The tunneling coupling $J_{\rm SC}$ arises from a finite overlap of the wave functions and characterizes the critical current $I_{\rm c}=e^*J_{\rm SC}/\hbar$. The time-evolution of the relative phase is produced by an external voltage $\mathcal{V}$ across the superconducting junction, while the role is played by the magnetic field difference $\Delta\mathcal{E}$, the magnon-magnon interactions Λ, and the nonlinear effect in magnon Josephson junctions. Therefore even without any magnetic field differences, ac magnon Josephson effects can be generated by the nonlinear effect under an initial population imbalance $z(0)\neq 0$. See Ref. [28] for the Gross-Pitaevskii[182] Hamiltonian of magnon condensates derived directly from the original spin Hamiltonian.

	Conventional superconductor[166]	Quasiequilibrium magnon condensate
Order parameter	$\langle c_{\mathbf{k}\uparrow}c_{-\mathbf{k}\downarrow}\rangle\neq 0$	$\langle a(t)\rangle=\sqrt{N_{\rm cond.}}e^{i\vartheta(t)}\neq 0$ with $d\vartheta/(dt)\neq 0$
Carrier	$e^*\equiv 2e$	$g\mu_{\rm B}$
ac and dc Josephson effects	Possible[73]:	Possible[28] (see Sec. IV C 2 for MQST):
Current Josephson Eq.	$\frac{d}{dt}\Delta\mathcal{N}(t)=(2J_{\rm SC}/\hbar)\sin\Delta\varphi(t)$	$\frac{dz}{d\mathcal{T}}=-\sqrt{1-z^2}\sin(\theta+\theta_{\text{A-C}})$
Phase Josephson Eq.	$\frac{d}{dt}\Delta\varphi(t)=-2e\mathcal{V}(t)/\hbar$	$\frac{d\theta}{d\mathcal{T}}=\Delta\mathcal{E}+\Lambda z+\frac{z}{\sqrt{1-z^2}}\cos(\theta+\theta_{\text{A-C}})$
Persistent current in Ring	Possible:	'Possible'[28,29] as long as in condensation:
	For[62] over 10^{10^7} s	For[32,150,151] about a few hundreds ns
Quantization in Ring:	$\Phi=p\Phi_0$:	$\phi=p\phi_0$:
(See Table II)	$\Phi\equiv\oint_{\rm Ring}\mathrm{d}\mathbf{l}\cdot\mathbf{A}$	$\phi\equiv\oint_{\rm Ring}\mathrm{d}\mathbf{l}\cdot(\mathbf{E}\times\mathbf{e}_z)$
	$\Phi_0\equiv hc/e^*$	$\phi_0\equiv hc^2/(g\mu_{\rm B})$

Assuming that a ring of radius R consists of the cylindrical wire whose cross-section is $\pi\rho_0^2$ with the radius ρ_0 as sketched in Fig. 13, the magnitude of the 'persistent' condensed magnon current in the ring becomes (see Ref. [28] for details)

$$\mid I_{\rm Ring}\mid=2\pi g\mu_{\rm B}\mid J/\hbar\mid S\rho_0^2 a n_{\rm cond.}\mid\sin[2a\phi/(R\phi_0)]\mid, \tag{57}$$

where $n_{\rm cond.}$ is the number density of condensed magnons. The condensed magnon current flows '*persistently*' as long as magnons are in condensation. Such a persistent current is possible since quasiequilibrium magnon condensates are not the ground state but a quasiequilibrium metastable state. Remember that any persistent currents in the ground state are forbidden by Bloch theorem[183] (see also Ref. [188] for it). We note that the current in the ring is not steady when the quantization condition [Eq. (54)] is not satisfied, but these non-steady variations of the current away from its nonequilibrium steady state are small, on the relative order of $1/p\ll 1$ (typically, $p\geq\mathcal{O}(10)$). This is in contrast to a superconducting ring where the magnetic field of the supercurrent itself compensates the variations.

We[29] point out the possibility that using microwave pumping, the condensed magnon current might flow 'persistently' even at finite temperatures. Dissipations arise at finite temperature. Such detrimental effects, however, can be compensated[138] by magnon injection through microwave pumping where the pumping rate is larger than the dissipative decay rate.

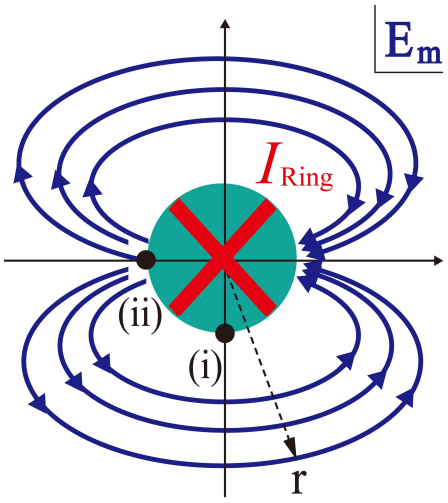

FIG. 14: (Color online) A schematic picture of the cross-section of the cylindrical wire in Fig. 13. The persistent condensed magnon current $I_{\rm Ring}$ in the ring produces the electric field $\mathbf{E}_{\rm m}(r)$, which leads to a measurable voltage difference $V_{\rm m}$ between the points (i) and (ii). Reprinted with permission from Ref. [28].

E. Electromagnetism of Magnon Current

Magnons (i.e., spins) are magnetic dipoles, which can be regarded[20] as a pair of oppositely charged magnetic monopoles of charge $\pm q_{\rm m}$ separated by a distance d in the limit $q_{\rm m}\to\infty$, $d\to 0$ with $q_{\rm m}d=g\mu_{\rm B}$ fixed. Taking this into account, Maxwell's equation can be formally enlarged. Thus, based on the resulting correspondence between electricity and magnetism, we theoretically pro-

TABLE VI: Electromagnetism[20,21,28] of the magnon current $I_{\rm Ring}$ in the cylindrical wire (see Figs. 13 and 14). A steady electron current produces a static magnetic field $B(r)$, while a steady spin current (*e.g.*, the persistent condensed magnon current $I_{\rm Ring}$ in the ring) generates a static electric field $E_{\rm m}(r)$, which results in the voltage drop $V_{\rm m}$ between the points (i) and (ii) in Fig. 14.

	Electron current $I_{\rm e}$	Magnon current $I_{\rm Ring}$
Carrier	e	$g\mu_{\rm B}$
Driving forces	Electric field and temperature gradient	Magnetic field gradient[120] and temperature gradient
Ampere′s law	$B(r)=I_{\rm e}/(2\pi r)$	$E_{\rm m}(r)=\mu_0 I_{\rm Ring}/(2\pi r^2)$
Ohm′s law	$V=RI_{\rm e}$	$V_{\rm m}\approx\mu_0 I_{\rm Ring}/(2\pi r)$

posed how to directly measure magnon currents without converting them into charge currents by the inverse spin Hall effect[39–41,43,63,67,189].

As is well-known, a steady charge current produces a static magnetic field. By contrast, the electromagnetic consequence of a steady spin current is a static electric field (Table VI). Spin currents produce two electric fields, one from the monopole and the other from the antimonopole. Each magnetic monopole current produces a static, asymptotically dipolar, electric field. Combining these two fields and taking the limit $d\to 0$, the resulting electric fields $\mathbf{E}_{\rm m}$ from magnon currents are shown in Fig. 14 for the cylindrical wire (Fig. 13) as an example. The magnitude[21] can be estimated by

$$|\mathbf{E}_{\rm m}(r)|=\frac{\mu_0}{2\pi r^2}\mid I_{\rm Ring}\mid, \tag{58}$$

which results in the voltage difference $V_{\rm m}$ between the points (i) and (ii). Within experimentally realizable sample values, it can amount to the nV range for condensed magnon currents, while to the mV range for noncondensed magnon currents (see Refs. [28] and [30] for details). Although small, such values are within experimental reach. We remark that the resulting voltage drop from noncondensed magnon is about 10^6 times larger than the one from condensed magnons since at room temperatures, the number density of noncondensed magnons is indeed[32] much larger than that of condensed magnons (Table IV).

V. CONCLUDING REMARKS

Using the spin-wave picture, we have classified magnon states in terms of their off-diagonal long-range order and reviewed their resulting transport properties in insulating magnets. Despite their different statistics, we found many phenomena analogous to electron transport in metals: a Wiedemann-Franz law for magnon transport, some Onsager reciprocal relation between the magnon Seebeck and Peltier coefficients, Hall effects of magnons, a quasiequilibrium magnon condensation, the ac and dc magnon Josephson effects, a quantized persistent current in Aharonov-Casher effects, a magnetic analog of a quantum RC circuit, magnon transistors, *etc.* Experimentally observing these phenomena would undoubtedly constitute milestones in this research area. We believe these goals are within reach using the present experimental techniques[32,92,150,151,156,168,190,191].

VI. OUTLOOK

Toward the next step of magnonics[33–38], we enumerate fundamental open issues and provide some perspectives.

A. Genuine Quantum Nature of Magnon

According to their bosonic nature magnons can form condensate and using microwave pumping, it can be realized also as a metastable state[32,138,150,151,153–155] even at room temperature; applying microwave, the system is driven into a nonequilibrium steady state and the zero-mode of magnons continues to be injected. After switching off the microwave, toward the true lowest energy state, the system undergoes a thermalization (i.e., relaxation) process subject to magnon-magnon interactions and thereby reaches a metastable state where the pumped magnons form condensate. Such dynamic or kinetic condensation in quasiequilibrium might be viewed as a *classical* phenomenon[152] due to the coupling with a thermal bath (i.e., thermally activated lattice vibration)[135,192,193]; applying a microwave, spins precess coherently and behave like a macroscopic spin. Since such a macroscopic object is subject to thermal bath, the relaxation and *decoherence* time[135,194,195] of a quantum superposition of macroscopically distinct states becomes extremely short at room temperature and it loses the quantum-mechanical properties in an extremely short time. The dynamics thus might be well described[152] by Landau-Lifshitz-Gilbert equation[196]. One may therefore wonder how to test and probe genuine quantum-mechanical properties[61,195] such as the *quantum coherence*[194] of such a macroscopic object. As to quantum coherence[197] effects in mesoscopic spin systems, see Refs. [61,88,195] and Ref. [175] for those in the dilute atomic alkali gases.

As a theoretical perspective[135,192,193] we note that, at finite temperatures, lattice vibrations become thermally activated and generally couple to spin degrees of freedom in solids. Partially tracing out the phonon degrees

of freedom from the spin-lattice interaction, the spin dynamics becomes being described by a reduced action and generally exhibits a non-unitary time-evolution (i.e. dissipation). That is, as long as phonons are alive, dissipations and the decoherence are inevitable in solids. How to overcome such detrimental effects and go beyond magnon injection by microwave pumping[29]? The conventional superconductors solve this issue by absorbing phonon degrees of freedom to form Cooper pairs. Could a similar mechanism be possible here? Isolated quantum system[198–201] (i.e., low temperature) might offer a platform to explore the possibility of genuine quantum-mechanical condensation[202].

B. Dirac Magnons

Magnons with a quadratic dispersion relation are identified with nonrelativistic-like magnons, while those with a linear dispersion can be viewed as relativistic-like magnons. On cubic lattices, the magnetization of FMs is characterized by nonrelativistic-like magnons contrary to AFs which have relativistic-like magnon excitations. Fransson *et al.*[203] have recently found that such a relativistic-like magnon can emerge from the geometric properties of honeycomb lattices (i.e., bipartite lattices) both in FMs and AFs. In analogy with Dirac fermions in graphene[204], the relativistic-like magnons are described by a magnon Dirac equation and may be called *Dirac magnons* (see Ref. [203] for details). Though their quantum-statistical properties are different, some analogous phenomena to Dirac fermions are still expected to emerge in Dirac magnon systems. Finding intrinsic relativistic effects associated with Dirac magnons transport is desired.

To this end, one of the promising platforms is quantum Hall systems[55]. The Hall conductivity of nonrelativistic-like fermions is[205,206] $\sigma_{xy} = -(e^2/h)\nu$ with Chern number $\nu \in \mathbb{Z}$, while that of Dirac fermions becomes[207] $\sigma_{xy}^{\rm Dirac} = -(2e^2/h)(2\nu+1)$ due to the quantum anomaly[208–210] of the lowest Landau level (*e.g.*, which makes the integer quantum Hall effect in graphene unconventional[211,212]). Both Hall conductivity become discrete. Thus, quantum Hall effects are characterized by a topological invariant, a Chern number, associated with the Berry curvature. Since the underlying Berry curvature[25,94,95,122–128,213] is a local quantity that reflects the geometric properties of the Bloch wavevector-space, it can be expected that quantum Hall effects emerge also in magnonic systems. A Landau level is[31] formed also in Dirac magnon systems. Taking that into account to exploit quantum Hall effects of Dirac magnons and to reveal their relativistic effects (*e.g.*, quantum anomaly) via magnon transport is certainly an interesting future direction[214]. A similar approach[215] will be useful to investigate the transport properties of *Weyl magnons*[216].

C. Optomagnonics

With the recent demonstration of the coherent coupling to a superconducting qubit in Ref. [217], hybrid structures involving the coherent coupling between insulating magnets with photonic[218–221] and electronic degrees of freedom has certainly a bright future.

Acknowledgments

We (KN and DL) acknowledge support by the Swiss National Science Foundation and the NCCR QSIT and by the JSPS (KN: Fellow No. 26-143). Many results reviewed in this article have been obtained in collaboration with a number of colleagues over the past years. In particular, it is a special pleasure to express our thanks to Kevin van Hoogdalem, Jelena Klinovaja, and Yaroslav Tserkovnyak for their valuable contributions.

[1] Y. Nambu and G. Jona-Lasinio, Phys. Rev. **122**, 345 (1961).
[2] J. Goldstone, Nuovo Cimento **19**, 154 (1961).
[3] J. Goldstone, A. Salam, and S. Weinberg, Phys. Rev. **127**, 965 (1962).
[4] Y. Nambu, J. Stat. Phys. **115**, 7 (2004).
[5] M. E. Peskin and D. V. Schroeder, *An Introduction To Quantum Field Theory* (Westview Press, 1995).
[6] S. Coleman, *Aspects of Symmetry* (Cambridge University Press, 1988).
[7] A. Altland and B. Simons, *Condensed Matter Field Theory* (Cambridge University Press, 2006).
[8] T. Brauner, Symmetry **2**, 609 (2010).
[9] H. Watanabe and H. Murayama, Phys. Rev. Lett. **108**, 251602 (2012).
[10] Y. Hidaka, Phys. Rev. Lett. **110**, 091601 (2013).
[11] F. Bloch, Z. Physik **61**, 206 (1930).
[12] T. Holstein and H. Primakoff, Phys. Rev. **58**, 1098 (1940).
[13] N. D. Mermin and H. Wagner, Phys. Rev. Lett. **17**, 1133 (1966).
[14] P. C. Hohenberg, Phys. Rev. **158**, 383 (1967).
[15] D. Loss, F. L. Pedrocchi, and A. J. Leggett, Phys. Rev. Lett. **107**, 107201 (2011).
[16] S. Tomonaga, Prog. Theor. Phys. **5**, 544 (1950).
[17] J. M. Luttinger, J. Math. Phys. **4**, 1154 (1963).
[18] D. Loss, P. Goldbart, and A. V. Balatsky, Phys. Rev. Lett. **65**, 1655 (1990).
[19] D. Loss and P. M. Goldbart, Phys. Rev. B **45**, 13544 (1992).
[20] D. Loss and P. M. Goldbart, Phys. Lett. A **215**, 197 (1996).
[21] F. Meier and D. Loss, Phys. Rev. Lett. **90**, 167204 (2003).
[22] B. Trauzettel, P. Simon, and D. Loss, Phys. Rev. Lett. **101**, 017202 (2008).
[23] K. A. van Hoogdalem, M. Albert, P. Simon, and D. Loss, Phys. Rev. Lett. **113**, 037201 (2014).

[24] K. A. van Hoogdalem and D. Loss, Phys. Rev. B **88**, 024420 (2013).
[25] K. A. van Hoogdalem, Y. Tserkovnyak, and D. Loss, Phys. Rev. B **87**, 024402 (2013).
[26] K. A. van Hoogdalem and D. Loss, Phys. Rev. B **84**, 024402 (2011).
[27] K. A. van Hoogdalem and D. Loss, Phys. Rev. B **85**, 054413 (2012).
[28] K. Nakata, K. A. van Hoogdalem, P. Simon, and D. Loss, Phys. Rev. B **90**, 144419 (2014).
[29] K. Nakata, P. Simon, and D. Loss, Phys. Rev. B **92**, 014422 (2015).
[30] K. Nakata, P. Simon, and D. Loss, Phys. Rev. B **92**, 134425 (2015).
[31] K. Nakata, J. Klinovaja, and D. Loss, to be submitted.
[32] S. O. Demokritov, V. E. Demidov, O. Dzyapko, G. A. Melkov, A. A. Serga, B. Hillebrands, and A. N. Slavin, Nature **443**, 430 (2006).
[33] A. V. Chumak, V. I. Vasyuchka, A. A. Serga, and B. Hillebrands, Nat. Phys. **11**, 453 (2015).
[34] A. Hoffmann and S. D. Bader, Phys. Rev. Applied **4**, 047001 (2015).
[35] A. A. Serga, A. V. Chumak, and B. Hillebrands, J. Phys. D **43**, 264002 (2010).
[36] G. E. W. Bauer, E. Saitoh, and B. J. van Wees, Nat.Mater **11**, 391 (2012).
[37] R. L. Stamps, S. Breitkreutz, J. Akerman, A. V. Chumak, Y. Otani, G. E. W. Bauer, J.-U. Thiele, M. Bowen, S. A. Majetich, M. Klaui, et al., J. Phys. D: Appl. Phys. **47**, 333001 (2014).
[38] G. E. W. Bauer, A. H. MacDonald, and S. Maekawa, Solid State Commun. **150**, 459 (2010).
[39] K. Uchida, S. Takahashi, K. Harii, J. Ieda, W. Koshibae, K. Ando, S. Maekawa, and E. Saitoh, Nature **455**, 778 (2008).
[40] K. Uchida, J. Xiao, H. Adachi, J. Ohe, S. Takahashi, J. Ieda, T. Ota, Y. Kajiwara, H. Umezawa, H. Kawai, et al., Nat. Mater. **9**, 894 (2010).
[41] K. Uchida, H. Adachi, T. An, T. Ota, M. Toda, B. Hillebrands, S. Maekawa, and E. Saitoh, Nat.Mater **10**, 737 (2011).
[42] J. Flipse, F. K. Dejene, D. Wagenaar, G. E. Bauer, J. B. Youssef, and B. J. van Wees, Phys. Rev. Lett. **113**, 027601 (2014).
[43] E. Saitoh, M. Ueda, H. Miyajima, and G. Tatara, Appl. Phys. Lett. **88**, 182509 (2006).
[44] F. K. Dejene, J. Flipse, and B. J. van Wees, Phys. Rev. B **90**, 180402(R) (2014).
[45] Y. Onose, T. Ideue, H. Katsura, Y. Shiomi, N. Nagaosa, and Y. Tokura, Science **329**, 297 (2010).
[46] H. Katsura, N. Nagaosa, and P. A. Lee, Phys. Rev. Lett. **104**, 066403 (2010).
[47] K. Tanabe, R. Matsumoto, J. Ohe, S. Murakami, T. Moriyama, D. Chiba, K. Kobayashi, and T. Ono, Appl. Phys. Express **7**, 053001 (2014).
[48] A. Klümper and K. Sakai, J. Phys. A **35**, 2173 (2002).
[49] S. Furukawa, D. Ikeda, and K. Sakai, J. Phys. Soc. Jpn. **74**, 3241 (2005).
[50] M. Filippone, F. Hekking, and A. Minguzzi, Phys. Rev. A **93**, 011602(R) (2016).
[51] R. Mahajan, M. Barkeshli, and S. A. Hartnoll, Phys. Rev. B **88**, 125107 (2013).
[52] N. Wakeham, A. F. Bangura, X. Xu, J.-F. Mercure, M. Greenblatt, and N. E. Hussey, Nat. Commun. **2**, 396 (2011).
[53] A. Garg, D. Rasch, E. Shimshoni, and A. Rosch, Phys. Rev. Lett. **103**, 096402 (2009).
[54] M.-R. Li and E. Orignac, Europhys. Lett. **60**, 432 (2002).
[55] See Ref. [222] for a violation of the free-electron Wiedemann-Franz law (i.e., Lorenz ratio) in fractional quantum Hall effects.
[56] D. Hirobe, M. Sato, T. Kawamata, Y. Shiomi, K. Uchida, R. Iguchi, Y. Koike, S. Maekawa, and E. Saitoh, Nat. Phys. **10.1038**, 3895 (2016).
[57] R. Cheng, S. Okamoto, and D. Xiao, arXiv:1606.01952.
[58] V. A. Zyuzin and A. A. Kovalev, arXiv:1606.03088.
[59] T. Jungwirth, X. Marti, P. Wadley, and J. Wunderlich, Nat. Nanotechnol. **11**, 231 (2016).
[60] S. Seki, T. Ideue, M. Kubota, Y. Kozuka, R. Takagi, M. Nakamura, Y. Kaneko, M. Kawasaki, and Y. Tokura, Phys. Rev. Lett. **115**, 266601 (2015).
[61] D. Loss, *Dynamical Properties of Unconventional Magnetic Systems* (NATO ASI Series E, A. T. Skjeltorp and D. Sherrington (eds.), Vol. 349, 1998, Kluwer, p. 29-75, 1998).
[62] C.Kittel, *Introduction to Solid State Physics* (Wiley, 8th edition, 2004).
[63] Y. Kajiwara, K. Harii, S. Takahashi, J. Ohe, K. Uchida, M. Mizuguchi, H. Umezawa, H. Kawai, K. Ando, K. Takanashi, et al., Nature **464**, 262 (2010).
[64] K. Uchida, H. Adachi, T. Kikkawa, A. Kirihara, M. Ishida, S. Yorozu, S. Maekawa, and E. Saitoh, arXiv:1604.00477.
[65] H. Adachi, J. Ohe, S. Takahashi, and S. Maekawa, Phys. Rev. B **83**, 094410 (2011).
[66] H. Adachi, K. Uchida, E. Saitoh, J. Ohe, S. Takahashi, and S. Maekawa, Apply. Phys. Lett. **97**, 252506 (2010).
[67] H. Adachi, K. Uchida, E. Saitoh, and S. Maekawa, Rep. Prog. Phys. **76**, 036501 (2013).
[68] J. Xiao, G. E. W. Bauer, K. Uchida, E. Saitoh, and S. Maekawa, Phys. Rev. B **81**, 214418 (2010).
[69] S. Hoffman, K. Sato, and Y. Tserkovnyak, Phys. Rev. B **88**, 064408 (2013).
[70] A. A. Kovalev and Y. Tserkovnyak, EPL **97**, 67002 (2012).
[71] R. Franz and G. Wiedemann, Annalen der Physik **165**, 497 (1853).
[72] An experimental realization of 'a magnon-supercurrent'[93,223,224] was reported in Ref. [168]. See Ref. [225] for superfluid in liquid ^{3}He.
[73] B. D. Josephson, Phys. Lett. **1**, 251 (1962).
[74] M. Büttiker, H. Thomas, and A. Prêtre, Phys. Lett. A **180**, 364 (1993).
[75] S. E. Nigg, R. López, and M. Büttiker, Phys. Rev. Lett. **97**, 206804 (2006).
[76] S. E. Nigg and M. Büttiker, Phys. Rev. B **77**, 085312 (2008).
[77] J. Gabelli, G. Fève, J. M. Berroir, and B. Placais, Rep. Prog. Phys. **75**, 126504 (2012).
[78] J. Gabelli, G. Fève, J. M. Berroir, B. Placais, A. Cavanna, B. Etienne, Y. Jin, and D. C. Glattli, Science **313**, 499 (2006).
[79] Y. Tserkovnyak, Nat. Nanotechnology **8**, 706 (2013).
[80] S. Datta, *Electronic Transpoer in Mesoscopic Systems* (Cambridge University Press, Cambridge, England, 1995).
[81] D. C. Mattis, *The Theory of Magnetism I* (Springer-Verlag, Berlin, 1981).
[82] T. Giamarchi, *Quantum Physics in One Dimension* (Oxford University Press, London, 2003).

[83] F. D. M. Haldane, Phys. Rev. Lett. **45**, 1358 (1980).
[84] I. Affleck, J. Phys. Condens. Matter **1**, 3047 (1989).
[85] E. Fradkin, *Field Theories of Condensed Matter Physics* (Cambridge University Press, Second edition, Cambridge, 2013).
[86] R. Mignani, J. Phys. A: Math. Gen. **24**, L421 (1991).
[87] X.-G. Hea and B. McKellarb, Phys. Lett. B **264**, 129 (1991).
[88] H.-B. Braun and D. Loss, Phys. Rev. B **53**, 3237 (1996).
[89] I. Dzyaloshinskii, J. Phys. Chem. Solids **4**, 241 (1958).
[90] T. Moriya, Phys. Rev. **120**, 91 (1960).
[91] T. Moriya, Phys. Rev. Lett. **4**, 228 (1960).
[92] X. Zhang, T. Liu, M. E. Flatte, and H. X. Tang, Phys. Rev. Lett. **113**, 037202 (2014).
[93] H. Katsura, N. Nagaosa, and A. V. Balatsky, Phys. Rev. Lett. **95**, 057205 (2005).
[94] A. Mook, J. Henk, and I. Mertig, Phys. Rev. B **91**, 224411 (2015).
[95] L. Zhang, J. Ren, J.-S. Wang, and B. Li, Phys. Rev. B **87**, 144101 (2013).
[96] Y. Aharonov and D. Bohm, Phys. Rev. **115**, 485 (1959).
[97] Y. Aharonov and A. Casher, Phys. Rev. Lett. **53**, 319 (1984).
[98] N. Gisin, G. Ribordy, W. Tittel, and H. Zbinden, Rev. Mod. Phys. **74**, 145 (2002).
[99] G. Fève, A. Mahé, J.-M. Berroir, T. Kontos, B. Plaçais, D. C. Glattli, A. Cavanna, B. Etienne, and Y. Jin, Science **316**, 1169 (2007), ISSN 0036-8075.
[100] A. Mahé, F. D. Parmentier, E. Bocquillon, J.-M. Berroir, D. C. Glattli, T. Kontos, B. Plaçais, G. Fève, A. Cavanna, and Y. Jin, Phys. Rev. B **82**, 201309 (2010).
[101] J. Dubois and et al., Nature **502**, 659 (2013).
[102] D. A. Ryndyk, *Theory of Quantum Transport at Nanoscale* (Springer International Publishing, Switzerland, 2015).
[103] G. B. Lesovik and I. A. Sadovskyy, Phys. Usp. **54**, 1007 (2011).
[104] J. Schwinger, J. Math. Phys **2**, 406 (1961).
[105] P. C. Martin and J. Schwinger, Phys. Rev. **115**, 1342 (1959).
[106] L. V. Keldysh, Sov. Phys. JETP **20**, 1018 (1965).
[107] J. Rammer, *Quantum Field Theory of Non-equilibrium States* (Cambridge University Press, Cambridge, 2007).
[108] H. Haug and A. Jauho, *Quantum Kinetics in Transport and Optics of Semiconductors* (Springer New York, 2007).
[109] A. Kamenev, *Field Theory of Non-Equilibrium Systems* (Cambridge University Press, 2011, arXiv:0412296).
[110] G. Tatara, H. Kohno, and J. Shibata, Physics Report **468**, 213 (2008).
[111] T. Kita, Prog. Theor. Phys. **123**, 581 (2010).
[112] D. A. Ryndyk, R. Gutierrez, B. Song, and G. Cuniberti, *Energy Transfer Dynamics in Biomaterial Systems* (Springer-Verlag, 2009, p213, arXiv:08050628).
[113] NAND gate, one of the universal gates for classical computation, is a two-bit gate that provides a logical 0 as outcome only if both the input bits are 1, while it yields a logical 1 otherwise.
[114] S. Gatteschi, R. Sessoli, and J. Villain, *Molecular Nanomagnets* (Oxford University Press, New York, 2007).
[115] R. Sessoli, D. Gatteschi, A. Caneschi, and M. A. Novak, Nature (London) **365**, 141 (1993).
[116] L. Thomas, F. Lionti, R. Ballou, D. Gatteschi, R. Sessoli, and B. Barbara, Nature (London) **383**, 145 (1996).
[117] J. R. Friedman, M. P. Sarachik, J. Tejada, and R. Ziolo, Phys. Rev. Lett. **76**, 3830 (1996).
[118] A. Ardavan, O. Rival, J. J. L. Morton, S. J. Blundell, A. M. Tyryshkin, G. A. Timco, and R. E. P. Winpenny, Phys. Rev. Lett. **98**, 057201 (2007).
[119] In Ref. [31], providing a topological description[205,206,213] of the classical magnon Hall effect[21] induced by the A-C phase, we discuss the condition for magnonic 'quantum' Hall conductivities characterized by Chern number associated with Berry curvature of Bloch wavevector and provide the condition for the magnonic WF law[30] to demonstrate the universality. See Ref. [120] for the magnonic quantized Hall conductivity by phase twist[226].
[120] F. D. M. Haldane and D. P. Arovas, Phys. Rev. B **52**, 4223 (1995).
[121] S. Fujimoto, Phys. Rev. Lett. **103**, 047203 (2009).
[122] R. Matsumoto and S. Murakami, Phys. Rev. Lett. **106**, 197202 (2011).
[123] R. Matsumoto and S. Murakami, Phys. Rev. B **84**, 184406 (2011).
[124] R. Shindou, R. Matsumoto, S. Murakami, and J. Ohe, Phys. Rev. B **87**, 174427 (2013).
[125] R. Shindou, J. Ohe, R. Matsumoto, S. Murakami, and E. Saitoh, Phys. Rev. B **87**, 174402 (2013).
[126] R. Shindou and J. Ohe, Phys. Rev. B **89**, 054412 (2014).
[127] A. Mook, J. Henk, and I. Mertig, Phys. Rev. B **90**, 024412 (2014).
[128] A. Mook, J. Henk, and I. Mertig, Phys. Rev. B **91**, 174409 (2015).
[129] T. Senthil and M. Levin, Phys. Rev. Lett. **110**, 046801 (2013).
[130] N. Majlis, *The Quantum Theory of Magnetism* (World Scientific Publishing Co., 2007).
[131] G. D. Mahan, *Many-Particle Physics* (Kluwer Academic, Plenum Publishers, Third edition, 2000).
[132] B. I. Halperin and P. C. Hohenberg, Phys. Rev. **188**, 898 (1969).
[133] R. J. Glauber, Phys. Letters **21**, 650 (1966).
[134] C. L. Mehta and E. C. G. Sudarshan, Phys. Letters **22**, 574 (1966).
[135] H.-P. Breuer and F. Petruccione, *The Theory of Open Quantum Systems* (Cambridge University Press, Oxford, 2002).
[136] P. Coleman, *Introduction to Many-Body Physics* (Cambridge University Press, Cambridge, 2015).
[137] A macroscopic number of magnons occupies a single or several states, which is called single or fragmented condensation, respectively. See Refs. [166,175] for details.
[138] Y. M. Bunkov and G. E. Volovik, *Novel Superfluids (Chapter IV); eds. K. H. Bennemann and J. B. Ketterson* (Oxford University Press, Oxford, 2013, arXiv:1003.4889).
[139] N. W. Ashcroft and N. D. Mermin, *Solid State Physics* (Brooks Cole, 1976).
[140] See Refs. [227–229] for a treatment of thermal gradient using Luttinger's appraoch[230].
[141] L. Onsager, Phys. Rev. **38**, 2265 (1931).
[142] H. B. G. Casimir, Rev. Mod. Phys. **17**, 343 (1945).
[143] D. Sánchez and M. Büttiker, Phys. Rev. Lett. **93**, 106802 (2004).
[144] Using Johnson-Silsbee approach[145] and the thermodynamics out-of-equilibrium, Refs. [146,147] have microscopically introduced a magnon chemical potential that takes a nonzero value only in nonequilibrium.
[145] M. Johnson and R. H. Silsbee, Phys. Rev. B **35**, 4959

(1987).
[146] V. Basso, E. Ferraro, A. Magni, A. Sola, M. Kuepferling, and M. Pasquale, Phys. Rev. B **93**, 184421 (2016).
[147] V. Basso, E. Ferraro, and M. Piazzi, arXiv:1607.03301.
[148] B. Jenčič and P. Prelovšek, Phys. Rev. B **92**, 134305 (2015).
[149] I. S. Tupitsyn, P. C. E. Stamp, and A. L. Burin, Phys. Rev. Lett. **100**, 257202 (2008).
[150] A. A. Serga, V. S. Tiberkevich, C. W. Sandweg, V. I. Vasyuchka, D. A. Bozhko, A. V. Chumak, T. Neumann, B. Obry, G. A. Melkov, A. N. Slavin, et al., Nat. Commun. **5**, 3452 (2014).
[151] P. Clausen, D. A. Bozhko, V. I. Vasyuchka, B. Hillebrands, G. A. Melkov, and A. A. Serga, Phys. Rev. B **91**, 220402 (2015).
[152] A. Rückriegel and P. Kopietz, Phys. Rev. Lett. **115**, 157203 (2015).
[153] V. I. Yukalov, Laser Phys. **22**, 1145 (2012).
[154] V. Zapf, M. Jaime, and C. D. Batista, Rev. Mod. Phys. **86**, 563 (2014).
[155] D. L. Mills, Phys. Rev. Lett. **98**, 039701 (2007).
[156] S. O. Demokritov, B. Hillebrands, and A. N. Slavin, Phys. Rep. **348**, 441 (2001).
[157] F. S. Vannucchi, Á. R. Vasconcellos, and R. Luzzi, Phys. Rev. B **82**, 140404(R) (2010).
[158] F. S. Vannucchi, Á. R. Vasconcellos, and R. Luzzi, Eur. Phys. J. B **86**, 463 (2013).
[159] S. Rezende, Phys. Rev. B **79**, 174411 (2009).
[160] J. Hick, T. Kloss, and P. Kopietz, Phys. Rev. B **86**, 184417 (2012).
[161] T. Kloss, A. Kreisel, and P. Kopietz, Phys. Rev. B **81**, 104308 (2010).
[162] R. E. Troncoso and Á. S. Núñez, J. Phys.: Condens. Matter **24**, 036006 (2012).
[163] A. I. Bugrij and V. M. Loktev, Low Temp. Phys. **33**, 37 (2007).
[164] See Refs. [138,153–155,161,166,223,231,232] for an issue of magnon condensates[32,150,151,233,234].
[165] Y. M. Bunkov, Usp. Fiz. Nauk **180**, 884 (2010).
[166] A. J. Leggett, *Quantum Liquids: Bose Condensation And Cooper Pairing in Condensed-Matter Systems* (Oxford University Press, 2006).
[167] I. Zapata, F. Sols, and A. J. Leggett, Phys. Rev. A **57**, R28 (1998).
[168] D. A. Bozhko, A. A. Serga, P. Clausen, V. I. Vasyuchka, F. Heussner, G. A. Melkov, A. Pomyalov, V. S. L'vov, and B. Hillebrands, Nat. Phys. **10.1038**, 3838 (2016).
[169] A. Smerzi, S. Fantoni, S. Giovanazzi, and S. R. Shenoy, Phys. Rev. Lett. **79**, 4950 (1997).
[170] S. Raghavan, A. Smerzi, S. Fantoni, and S. R. Shenoy, Phys. Rev. A **59**, 620 (1999).
[171] S. Giovanazzi, A. Smerzi, and S. Fantoni, Phys. Rev. Lett. **84**, 4521 (2000).
[172] M. Albiez, R. Gati, J. Fölling, S. Hunsmann, M. Cristiani, and M. K. Oberthaler, Phys. Rev. Lett. **95**, 010402 (2005).
[173] S. O. Demokritov, private communication.
[174] We note this is a rough estimation. More microscopic evaluation will be desired.
[175] A. J. Leggett, Rev. Mod. Phys. **73**, 307 (2001).
[176] S. Levy, E. Lahoud, I. Shomroni, and J. Steinhauer, Nature **449**, 579 (2007).
[177] R. E. Troncoso and Á. S. Núñez, Ann. Phys. **346**, 182 (2014).
[178] A. Schilling and H. Grundmann, Ann. Phys. **327**, 2301 (2012).
[179] Y. M. Bunkov, private communication.
[180] Y. M. Bunkov and G. E. Volovik, Phys. Rev. Lett. **98**, 265302 (2007).
[181] Y. M. Bunkov, V. V. Dmitriev, Y. M. Mukharskii, and G. Tvalashvili, Sov. Phys. JETP **67**, 300 (1988).
[182] J. Hick, F. Sauli, A. Kreisel, and P. Kopietz, Eur. Phys. J. B **78**, 429 (2010).
[183] N. Yamamoto, Phys. Rev. D **92**, 085011 (2015).
[184] N. Byers and C. N. Yang, Phys. Rev. Lett. **7**, 46 (1961).
[185] M. Büttiker, Y. Imry, and R. Landauer, Phys. Lett. **96A**, 365 (1983).
[186] F. Schütz, M. Kollar, and P. Kopietz, Phys. Rev. Lett. **91**, 017205 (2003).
[187] W. Chen, P. Horsch, and D. Manske, Phys. Rev. B **87**, 214502 (2013).
[188] H. Watanabe and M. Oshikawa, Phys. Rev. Lett. **114**, 251603 (2015).
[189] Y. Tserkovnyak, A. Brataas, G. E. W. Bauer, and B. I. Halperin, Rev. Mod. Phys. **77**, 1375 (2005).
[190] M. Agrawal, V. I. Vasyuchka, A. A. Serga, A. D. Karenowska, G. A. Melkov, and B. Hillebrands, Phys. Rev. Lett. **111**, 107204 (2013).
[191] S. R. Boona and J. P. Heremans, Phys. Rev. B **90**, 064421 (2014).
[192] A. Abragam, *Principles of Nuclear Magnetism* (Clarendon Press, Oxford, 1983).
[193] A. O. Caldeira and A. J. Leggett, Physica A **121**, 587 (1983).
[194] W. H. Zurek, Physics Today **44**, 36 (1991).
[195] M. N. Leuenberger, F. Meier, and D. Loss, Chemical Monthly **134**, 217 (2003).
[196] T. L. Gilbert, IEEE Transactions on Magnetics **40**, 3443 (2004).
[197] See also Ref. [225] for phase coherence in superfluid phases.
[198] S. Goldstein, T. Hara, and H. Tasaki, Phys. Rev. Lett. **111**, 140401 (2013).
[199] M. Gring, M. Kuhnert, T. Langen, T. Kitagawa, B. Rauer, M. Schreitl, I. Mazets, D. A. Smith, E. Demler, and J. Schmiedmayer, Science **337**, 1318 (2012).
[200] A. Lazarides, A. Das, and R. Moessner, Phys. Rev. Lett. **112**, 150401 (2014).
[201] H. Aoki, N. Tsuji, M. Eckstein, M. Kollar, T. Oka, and P. Werner, Rev. Mod. Phys. **86**, 779 (2014).
[202] See Ref. [235] for observation of the kinetic condensation of classical waves and Ref. [236] for theoretical analysis on Bose-Einstein condensation of overpopulated quark-gluon plasma.
[203] J. Fransson, A. M. Black-Schaffer, and A. V. Balatsky, Phys. Rev. B **94**, 075401 (2016).
[204] A. H. C. Neto, F. Guinea, N. M. R. Peres, K. S. Novoselov, and A. K. Geim, Rev. Mod. Phys. **81**, 109 (2009).
[205] D. J. Thouless, M. Kohmoto, M. P. Nightingale, and M. den Nijs, Phys. Rev. Lett. **49**, 405 (1982).
[206] M. Kohmoto, Ann. Phys. **160**, 343 (1985).
[207] V. P. Gusynin and G. Sharapov, Phys. Rev. Lett. **95**, 146801 (2005).
[208] K. Ishikawa, Phys. Rev. Lett. **53**, 1615 (1984).
[209] K. Ishikawa, Phys. Rev. D **31**, 1432 (1985).
[210] A. M. J. Schakel, Phys. Rev. D **43**, 1428 (1991).
[211] Y. Zhang, Y.-W. Tan, H. L. Stormer, and P. Kim, Nature

438, 201 (2005).
[212] K. S. Novoselov, A. K. Geim, S. V. Morozov, D. Jiang, M. I. Katsnelson, I. V. Grigorieva, S. V. Dubonos, and A. A. Firsov, Nature **438**, 197 (2005).
[213] D. Xiao, M.-C. Chang, and Q. Niu, Rev. Mod. Phys. **82**, 1959 (2010).
[214] As in Ref. [129], such approach from symmetry-protected topological phase[237] might be useful.
[215] K.-Y. Yang, Y.-M. Lu, and Y. Ran, Phys. Rev. B **84**, 075129 (2011).
[216] F.-Y. Li, Y.-D. Li, Y.-B. Kim, L. Balents, Y. Yu, and G. Chen, arXiv:1602.04288.
[217] Y. Tabuchi, S. Ichino, A. Noguchi, T. Ishikawa, R. Yamazaki, K. Usami, and Y. Nakamura, Science **349**, 405 (2015).
[218] A. Osada, R. Hisatomi, A. Noguchi, Y. Tabuchi, R. Yamazaki, K. Usami, M. Sadgrove, R. Yalla, M. Nomura, and Y. Nakamura, Phys. Rev. Lett. **116**, 223601 (2016).
[219] T. Liu, X. Zhang, H. X. Tang, , and M. E. Flatté, Phys. Rev. B **94**, 060405(R) (2016).
[220] S. V. Kusminskiy, H. X. Tang, and F. Marquardt, Phys. Rev. A **94**, 033821 (2016).
[221] M. Aspelmeyer, T. J. Kippenberg, and F. Marquardt, Rev. Mod. Phys. **86**, 1391 (2014).
[222] C. L. Kane and M. P. A. Fisher, Phys. Rev. B **55**, 15832 (1997).
[223] E. B. Sonin, Adv. Phys. **59**, 181 (2010).
[224] H. Skarsvag, C. Holmqvist, and A. Brataas, Phys. Rev. Lett. **115**, 237201 (2015).
[225] A. J. Leggett, Rev. Mod. Phys. **47**, 331 (1975).
[226] Q. Niu, D. J. Thouless, and Y.-S. Wu, Phys. Rev. B **31**, 3372 (1985).
[227] A. Shitade, Prog. Theor. Exp. Phys. **2014**, 123I01 (2014).
[228] G. Tatara, Phys. Rev. Lett. **114**, 196601 (2015).
[229] H. Kohno, Y. Hiraoka, M. Hatami, and G. E. W. Bauer, Phys. Rev. B **94**, 104417 (2016).
[230] J. M. Luttinger, Phys. Rev. **135**, A1505 (1964).
[231] D. Snoke, Nature **443**, 403 (2006).
[232] T. Giamarchi, C. Ruegg, and O. Tchernyshyov, Nat. Phys. **4**, 198 (2008).
[233] T. Nikuni, M. Oshikawa, A. Oosawa, and H. Tanaka, Phys. Rev. Lett. **84**, 5868 (2000).
[234] T. Radu, H. Wilhelm, V. Yushankhai, D. Kovrizhin, R. Coldea, Z. Tylcznski, T. Luhmann, and F. Steglich, Phys. Rev. Lett. **95**, 127202 (2005).
[235] C. Sun, S. Jia, C. Barsi, S. Rica, A. Picozzi, and J. W. Fleischer, Nat. Phys. **8**, 470 (2012).
[236] J.-P. Blaizot, F. Gelis, J. Liao, L. McLerran, and R. Venugopalan, Nucl. Phys. A **873**, 68 (2012).
[237] B. Zeng, X. Chen, D.-L. Zhou, and X.-G. Wen, arXiv:1508.02595.